EMP Theoretical Notes

Note 66
6 October 1969

Prompt Gamma Effects in a Homogeneous Atmosphere

Vernon W. Pine
Air Force Weapons Laboratory

ABSTRACT

One-dimensional, time-dependent photon transport is evaluated by the Monte Carlo method for a point source of gamma rays in a homogeneous air. The ionization rate and current are obtained in a region extending from the source to three kilometers from the source. Results are available for several gamma source energies from .5 to 8 MeV.

I. Introduction

In this report the results of a series of Monte Carlo calculations of gamma effects in a homogeneous air are presented. The direct beam quantities calculated are the energy deposited per unit volume and the total charge displacement per unit volume. Also the scattered beam current and energy deposition rates are calculated along with the associated buildup factors.

The spacial region of interest extends to 3000 meters or 10 mean free paths, whichever distance is closer to the source. There are 120 radial bins each 25 meters in width. The retarded time† region extends to .5 microseconds.

Results are available for monoenergetic gamma sources at .5, 1., 2., 3., 4., 5., 6., 7., and 8. MeV.

II. The Problem and Physics Used.

The air composition used in these runs is 77.10% nitrogen, 21.30% oxygen, 1.15% hydrogen and .45% argon. All results are for an air of uniform density at 0° centigrade and .76 mHg.

The allowable interactions for a photon are Compton scattering and pair production (if the incident photon energy is greater than 2.0 MeV). Photoelectric processes are not treated explicitly, i.e., photoelectric cross sections are not included in curve fits for the mean free path but are approximated by the lower energy cutoff treatment.

When a photon undergoes a pair event only one of the two photons subsequently created by position annihilation is followed and its relative weight is doubled. The annihilation photon is assumed to be emitted isotropically from the annihilation event.

When a photon undergoes a Compton interaction the energy of the scattered photon is determined by selecting a random number and interpolating from a table of scattered photon energy versus random numbers. The selection of scattered photon energy uniquely determines the scattered photon direction from the Klein-Nishina distribution. The electron energy used in scoring the collision effects is determined from a curve fit of the average electron recoil energy for the given incident photon energy.

When a photon's energy falls below 5% of the source energy, the remaining photon energy is deposited in the local bin and a new history is initiated. As can be seen from figures 27 through 29, the choice of cutoff energy can distort the time histories, especially for regions near the source. Previous studies on TIGRE indicate that the value chosen

† The retarded time at a point equals the real time minus the radial distance to that point divided by the speed of light.

for a lower cutoff energy (5%) did not appreciably alter the spacial distribution of energy deposition. In the present studies the temporal distortion within the first half microsecond was judged acceptable.

A cutoff energy of 5% of the initial energy of a photon emitted from the source is used for two reasons. First and foremost, one has to consider the way in which these results are used. Since these results are used as inputs to the EMP field codes, one notes that the radial current is not affected by the choice of cutoff energy. Only the energy deposition rates are altered significantly by the choice of cutoff energy. The energy deposition rate is used in calculating the conductivity and it is felt that the error contributed by the choice of the higher cutoff energy is acceptable in that it is far from the most uncertain element in the calculation of the conductivity (and the fields).

Secondly, one must consider the difference in computer time required to make a 1% cutoff run as opposed to a 5% run. With a 1% cutoff, approximately 1.2×10^4 histories/minute are calculated, while a 5% cutoff allows approximately 8.4×10^4 histories/minute to be calculated. Since each of the present runs consumes approximately 5 hours on the CDC 6600, it is not felt that the additional time is justified and, hence, the 5% cutoff has been used. In the future one might wish to reconsider this decision.

For these runs there are 120 radial bins each 25 meters in width. For each radial interval there are 19 time bins. The first 10 shakes[†] are divided into 10 bins, each 1 shake in width. The remaining bins are 5 shakes in width. In each of these bins, statistics are calculated on the current and energy deposition rates. No more than 5% of the bins in a given run have a statistical uncertainty greater than ± 15%.

In order to obtain this degree of statistical uncertainty in bins far removed from the source, in a reasonable number of histories, some form of variance reduction is needed. Biasing the path length to favor longer paths was the technique used in the present calculations. Accordingly the number of mean free paths is selected from

$$F = - (1. + .75 \cos^2 \theta) \log (1. - R)$$

where

F — The number of mean free paths to the next collision

θ — The angle between the radial to the previous collision and the photon direction

R — Random number

[†] 1 shake = 10^{-8} sec.

When θ is greater than 90° no stretching is allowed. When stretching occurs the score is weighted to remove the bias from the result.

III. Results of the Calculation

A complete presentation of the results is not practical due to the number of quantities calculated. Instead some typical results are given for source energies of 1., 4., and 8. MeV at approximately 1, 5, 10 mean free paths from the source. These results are presented in histogram form in figures 1 through 18. The entire results are contained on magnetic tape and microfilm.

The energy deposition buildup factor and the Compton current buildup factor plotted as functions of distance from the source appear in figures 19 through 24. Along with the energy deposition buildup factor curves, two sets of points are overlain. The first set gives the results from a moments method calculation by Goldstein and Wilkins.[1] The other set of points is from a Monte Carlo calculation by LeLevier.[2] The LeLevier points are in general lower than the present results because LeLevier discards the remaining energy of the photon when it falls below 5% of the source energy. Furthermore, LeLevier states that his cutoff procedure was chosen to obtain agreement with the Goldstein & Wilkins results. I chose to follow a more physically oriented procedure.

Figure 25 and figure 26 show the energy deposition rates and currents with the LeLevier data overlaid. Again LeLevier's results for the energy deposition rates at later times are lower than present results because of the difference in cutoff treatments.

Future plans are to curve fit these results for incorporation in EMP source codes.

REFERENCES

1. Goldstein, H., Fundamental Aspects of Reactor Shielding, Appendix D. New York: Addison-Wesley, 1959.

2. LeLevier, R. E., "The Compton Current and the Energy Deposition Rate from Gamma Quanta-A Monte Carlo Calculations," RAND Memorandum RM-4151-PR.

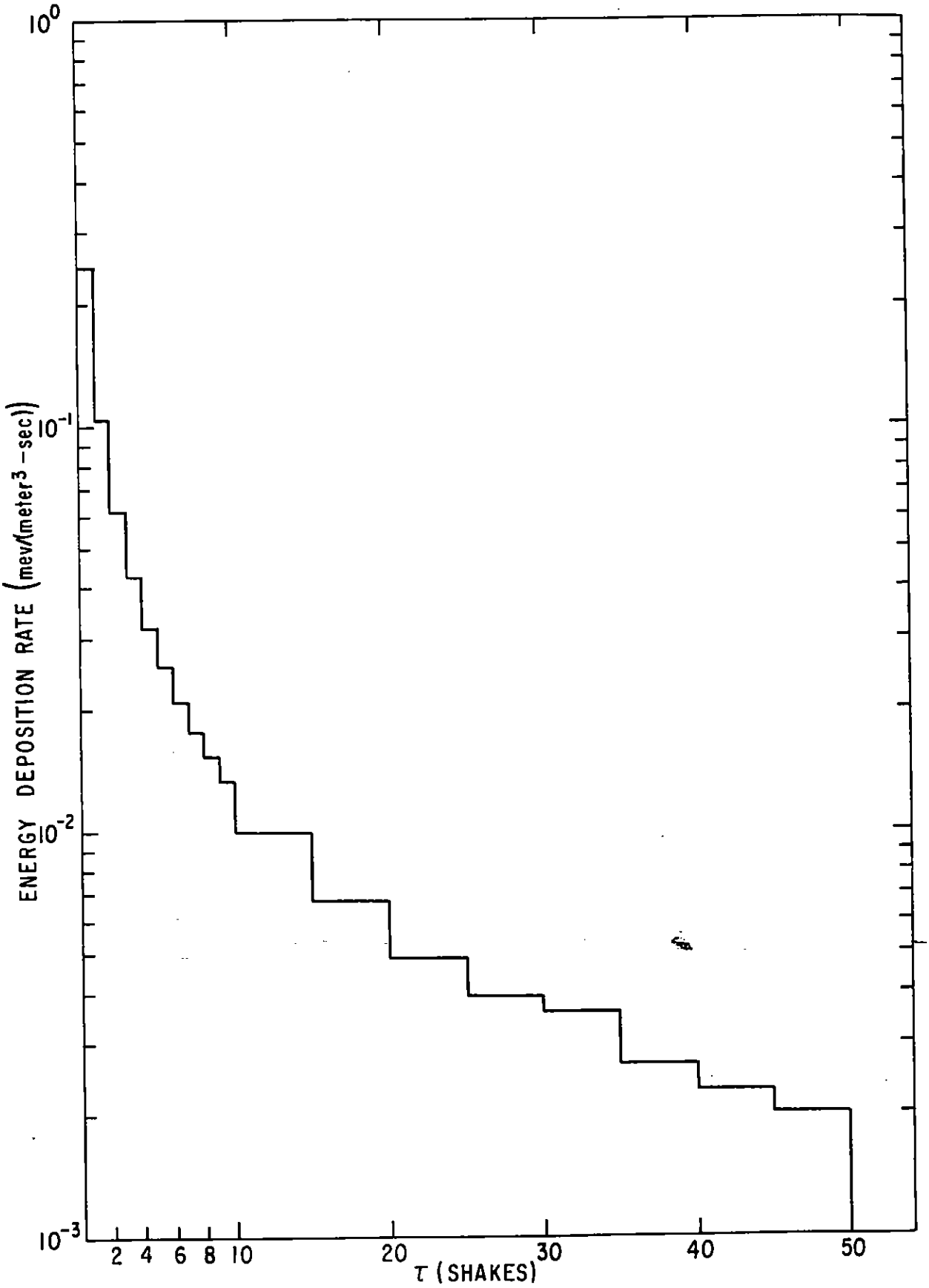

Fig. 1 Energy Deposition Rate for 1 Mev gammas at 112.50 meters (.95 m.f.p.)

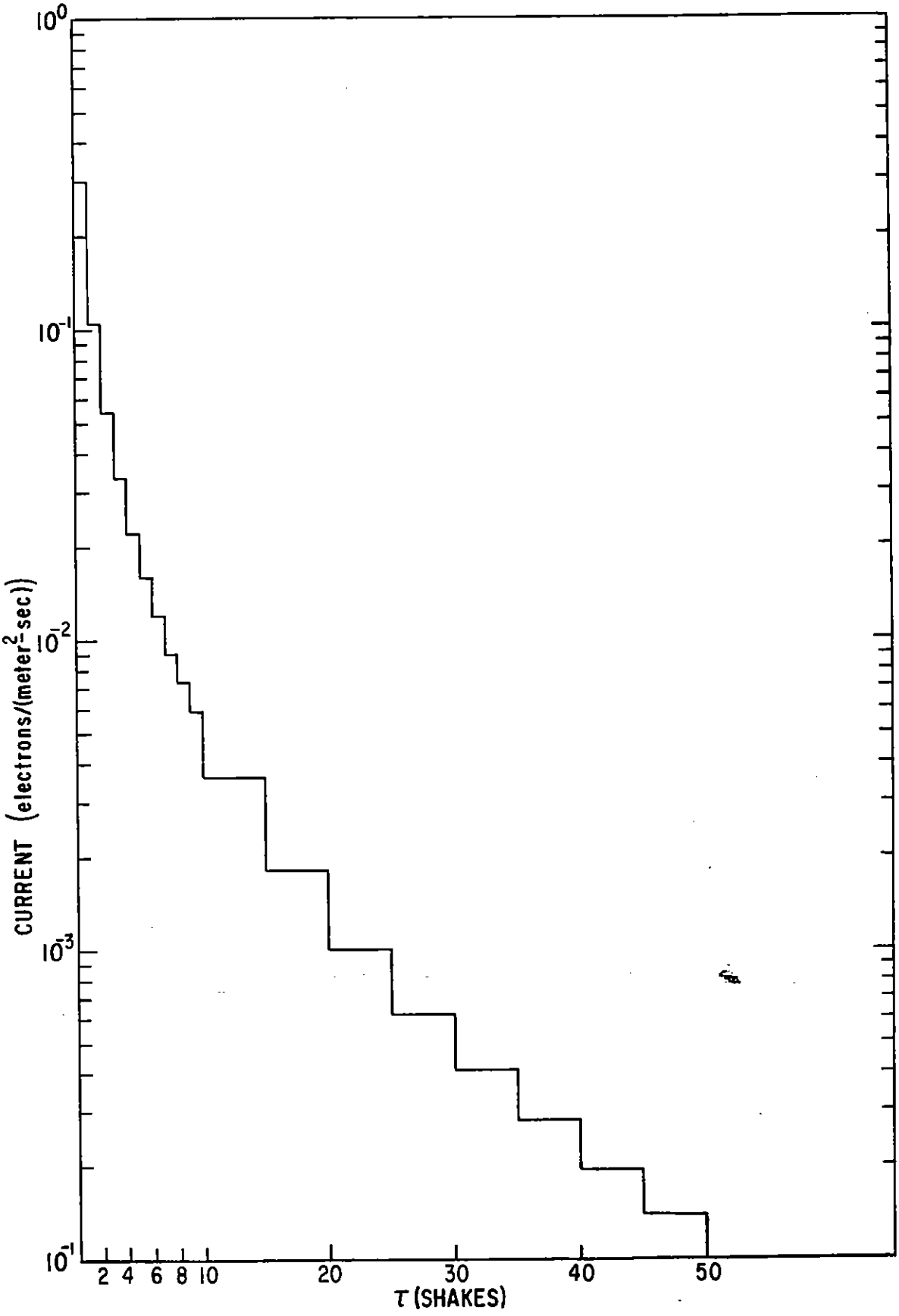

Fig. 2 Radial Current for 1 Mev gammas at 112.50 meters (.95 m.f.p.)

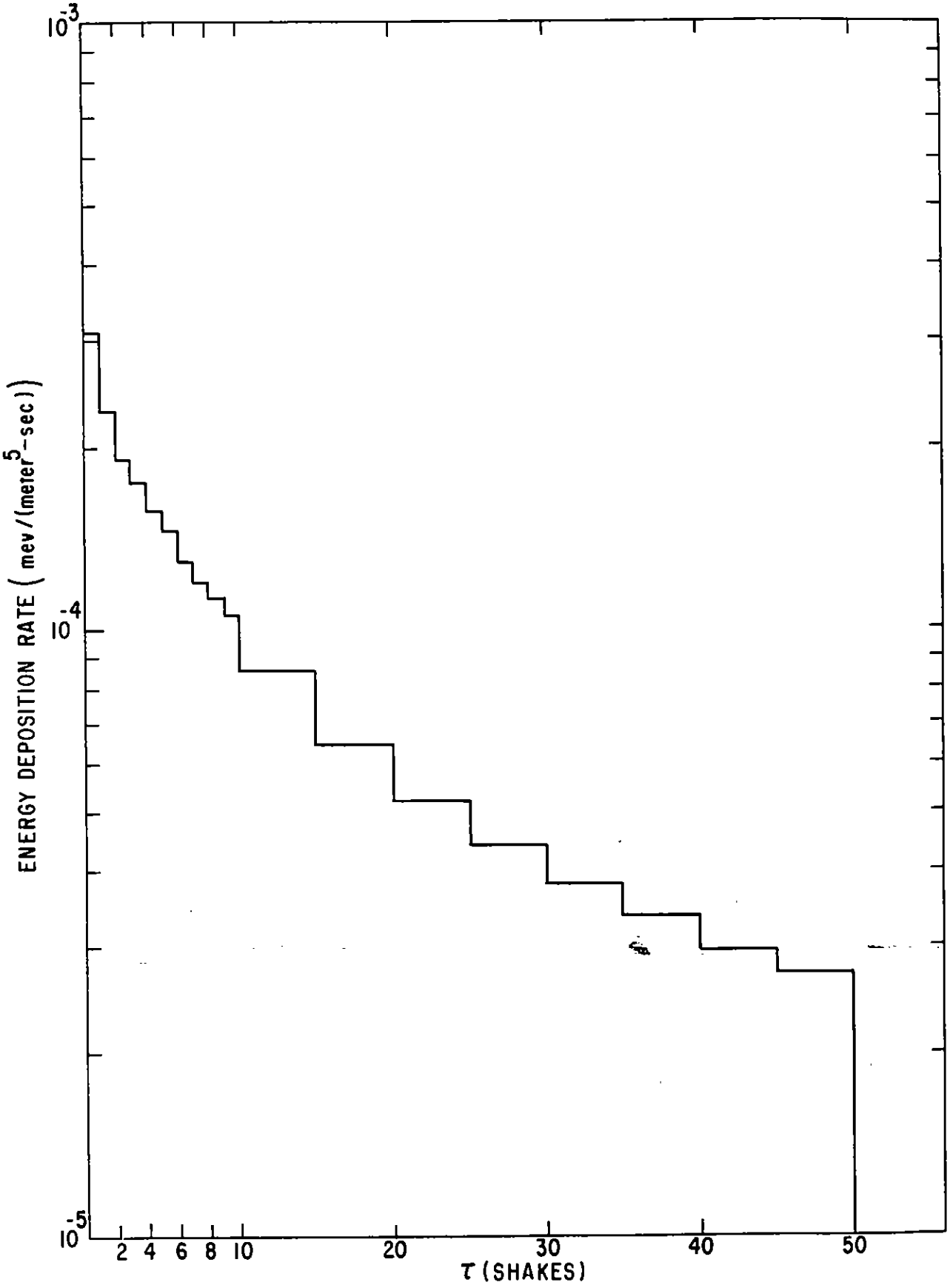

Fig. 3 Energy Deposition Rate for 1 Mev gammas at 587.50 meters (4.95 m.f.p.)

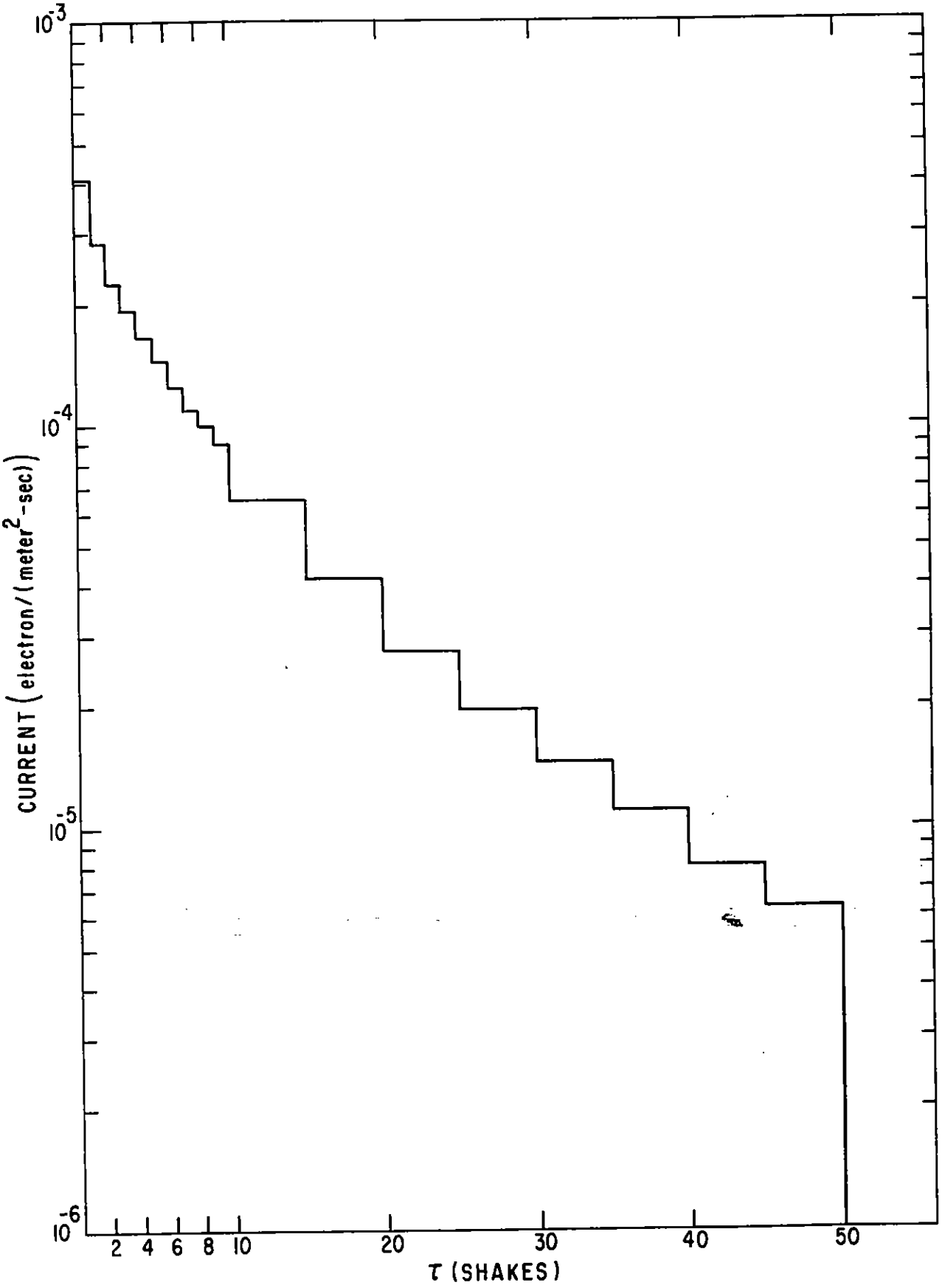

Fig. 4 Radial Current for 1 Mev gammas at 587.50 meters (4.95 m.f.p.)

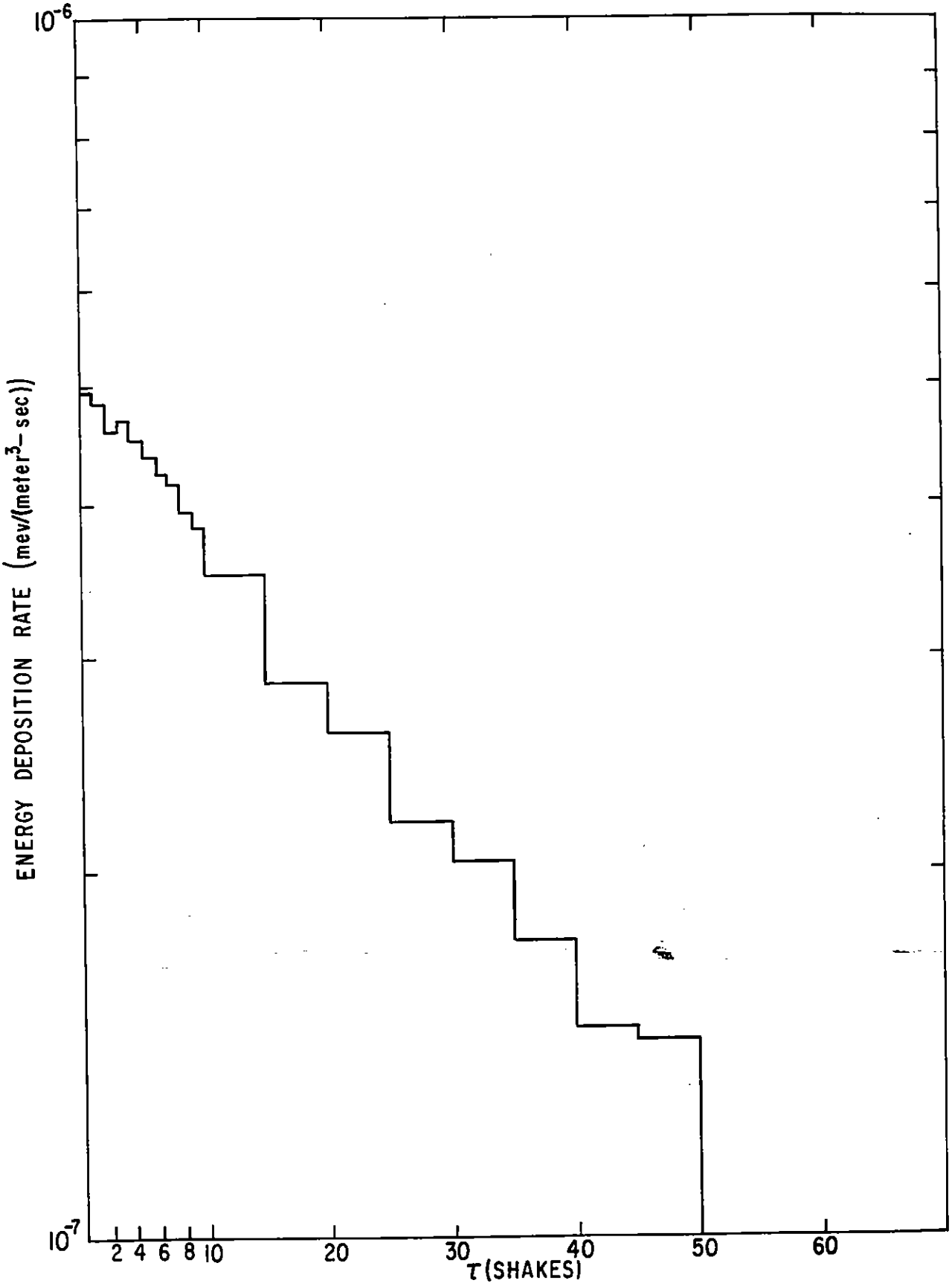

Fig. 5 Energy Deposition Rate for 1 Mev gammas at 1187.50 meters (10.01 m.f.p.)

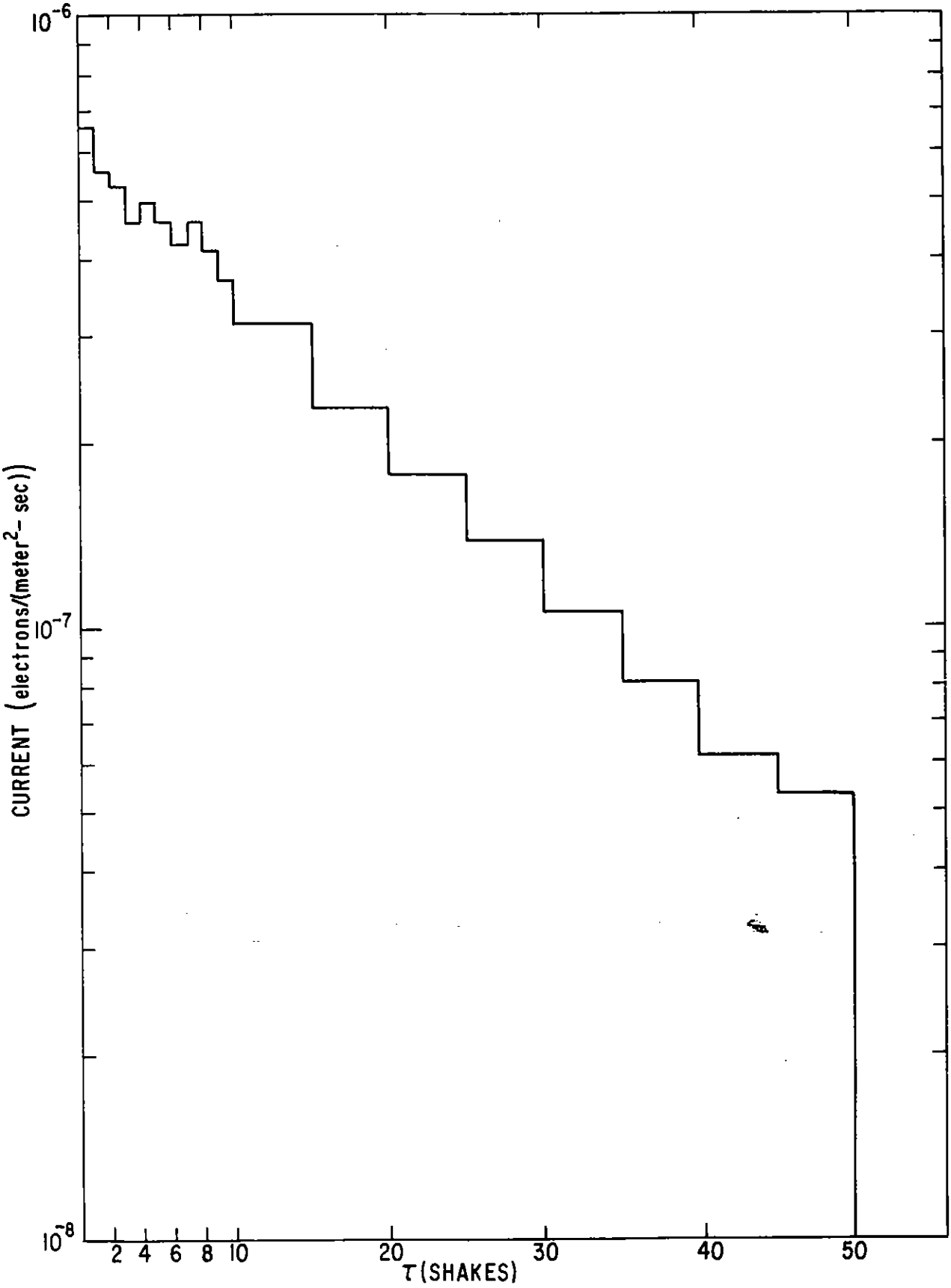

Fig. 6 Radial Current for 1 Mev gammas at 1187.50 meters (10.01 m.f.p.)

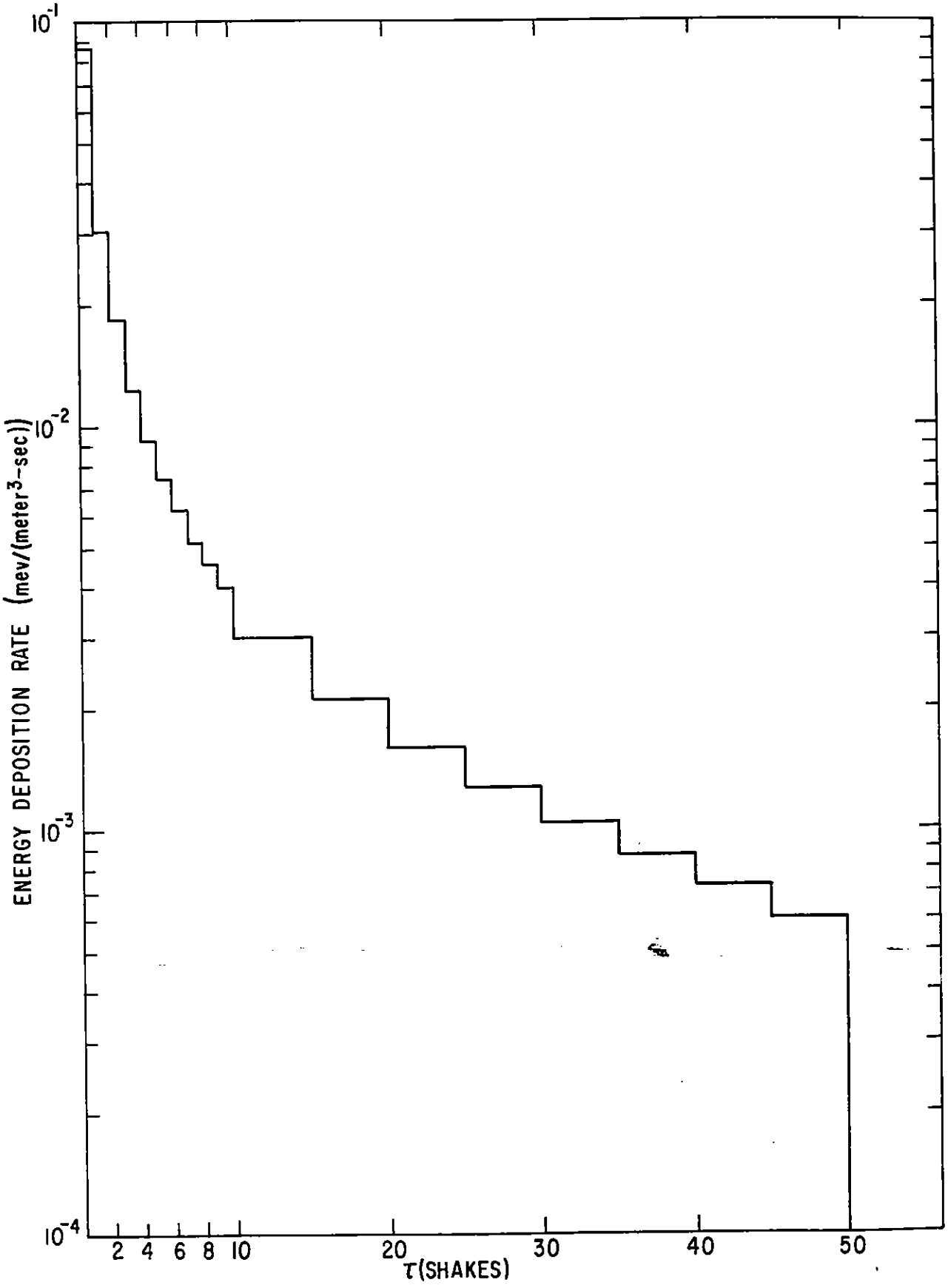

Fig. 7 Energy Deposition Rate for 4 Mev gammas at 262.50 meters (1.03 m.f.p.)

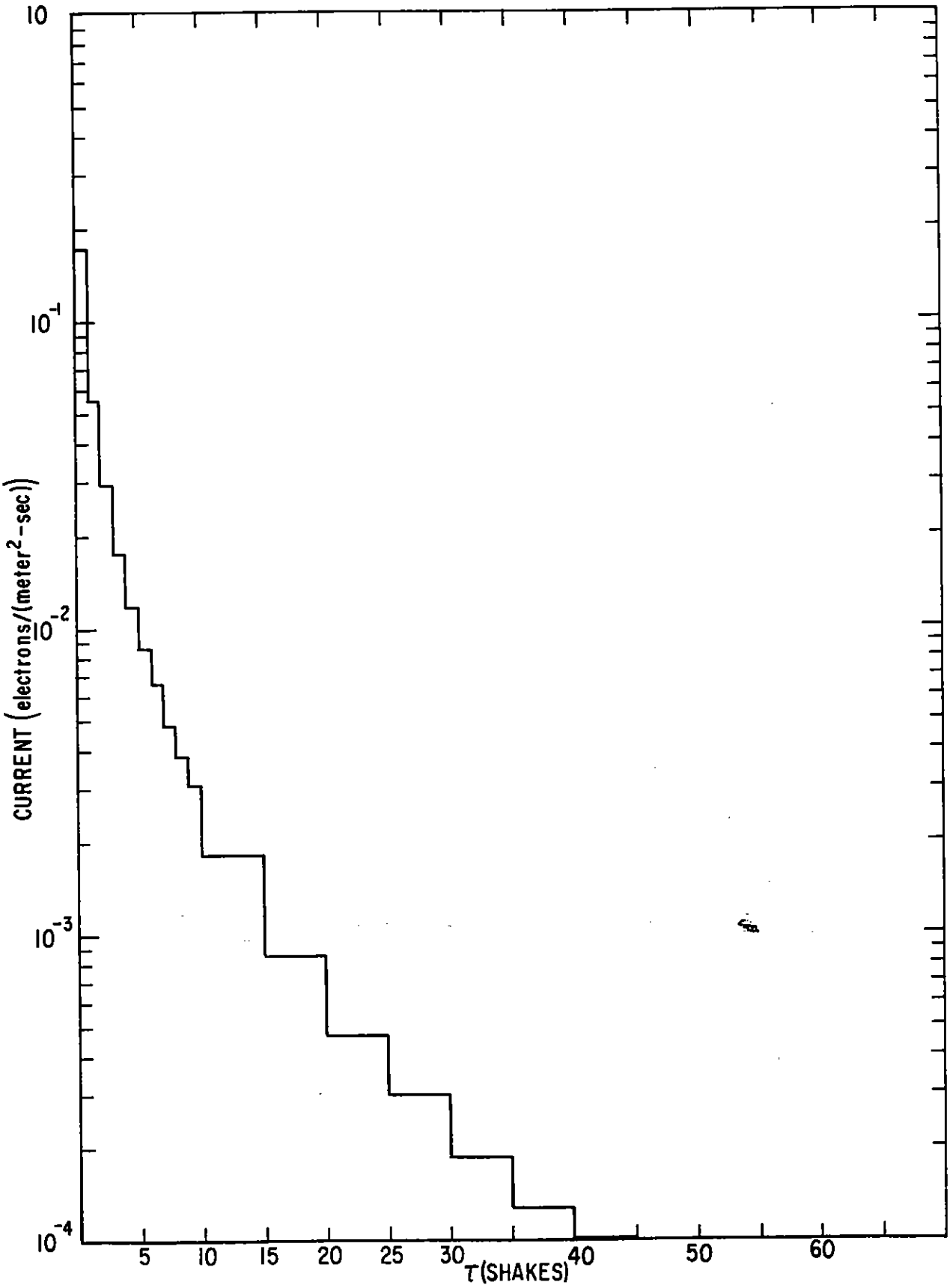

Fig. 8 Radial Current for 4 Mev gammas at 262.50 meters (1.03 m.f.p.)

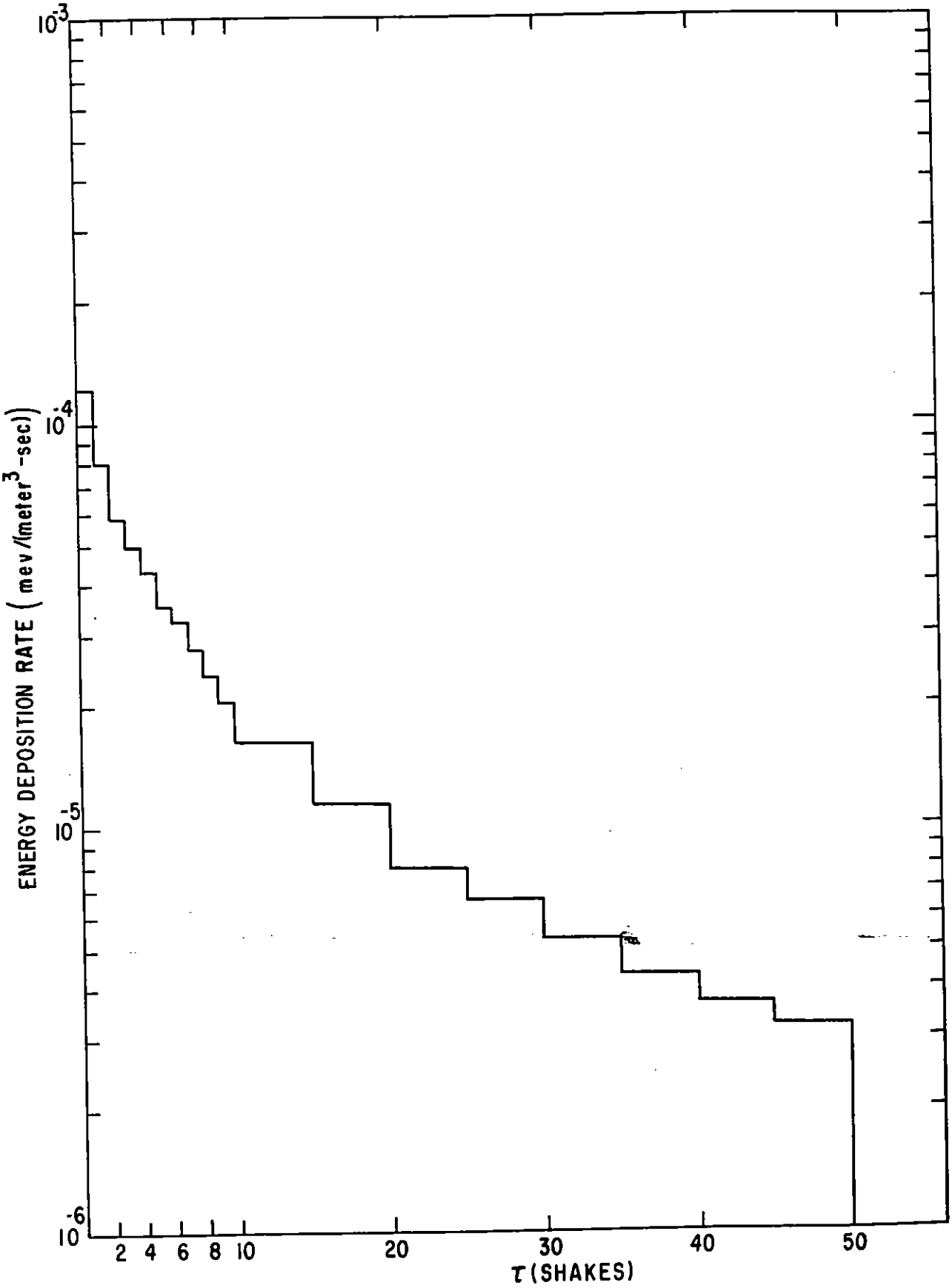

Fig. 9 Energy Deposition Rate for 4 Mev gammas at 1287.50 meters (5.03 m.f.p.)

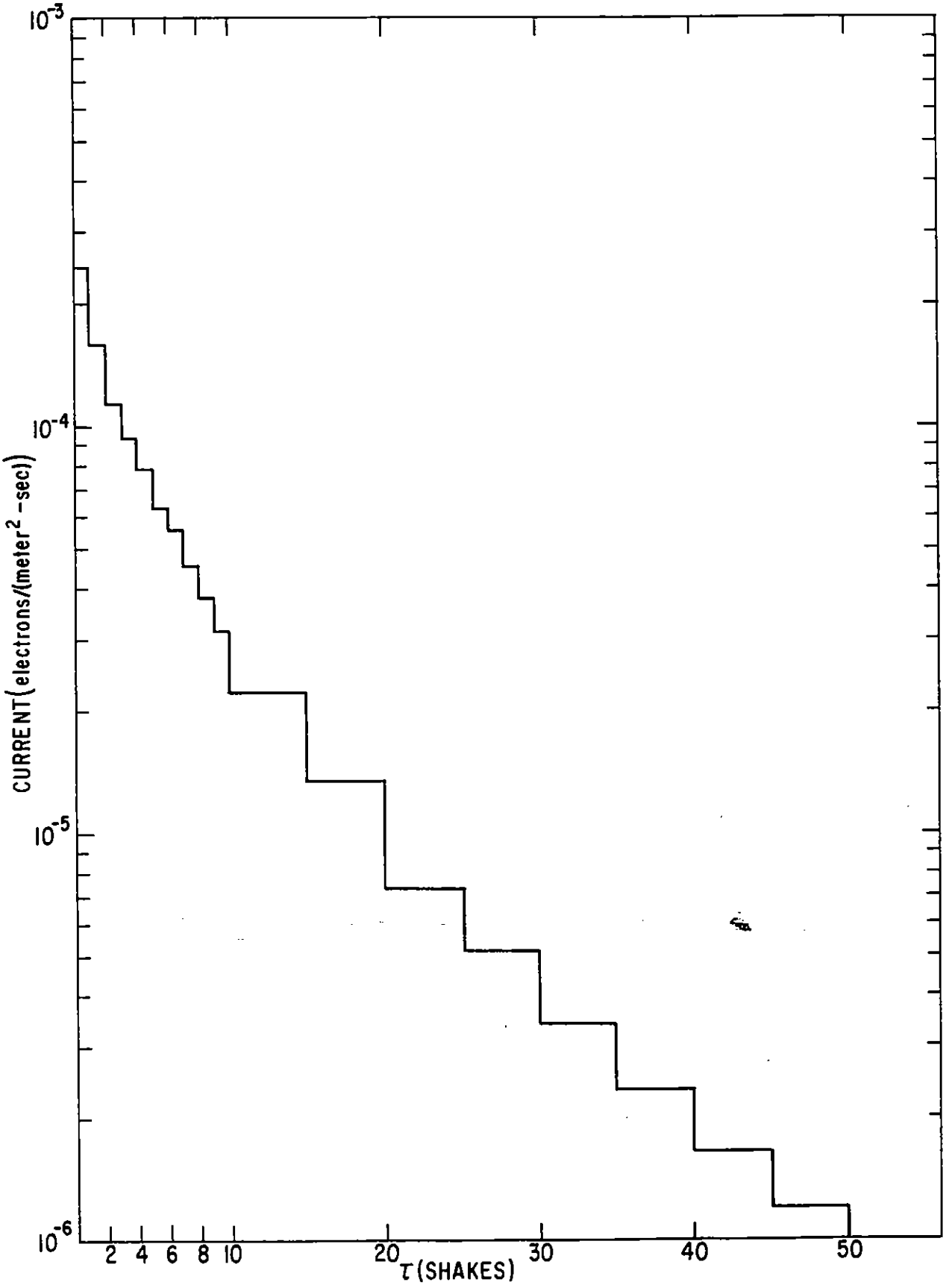

Fig. 10 Radial Current for 4 Mev gammas at 1287.50 meters (5.03 m.f.p.)

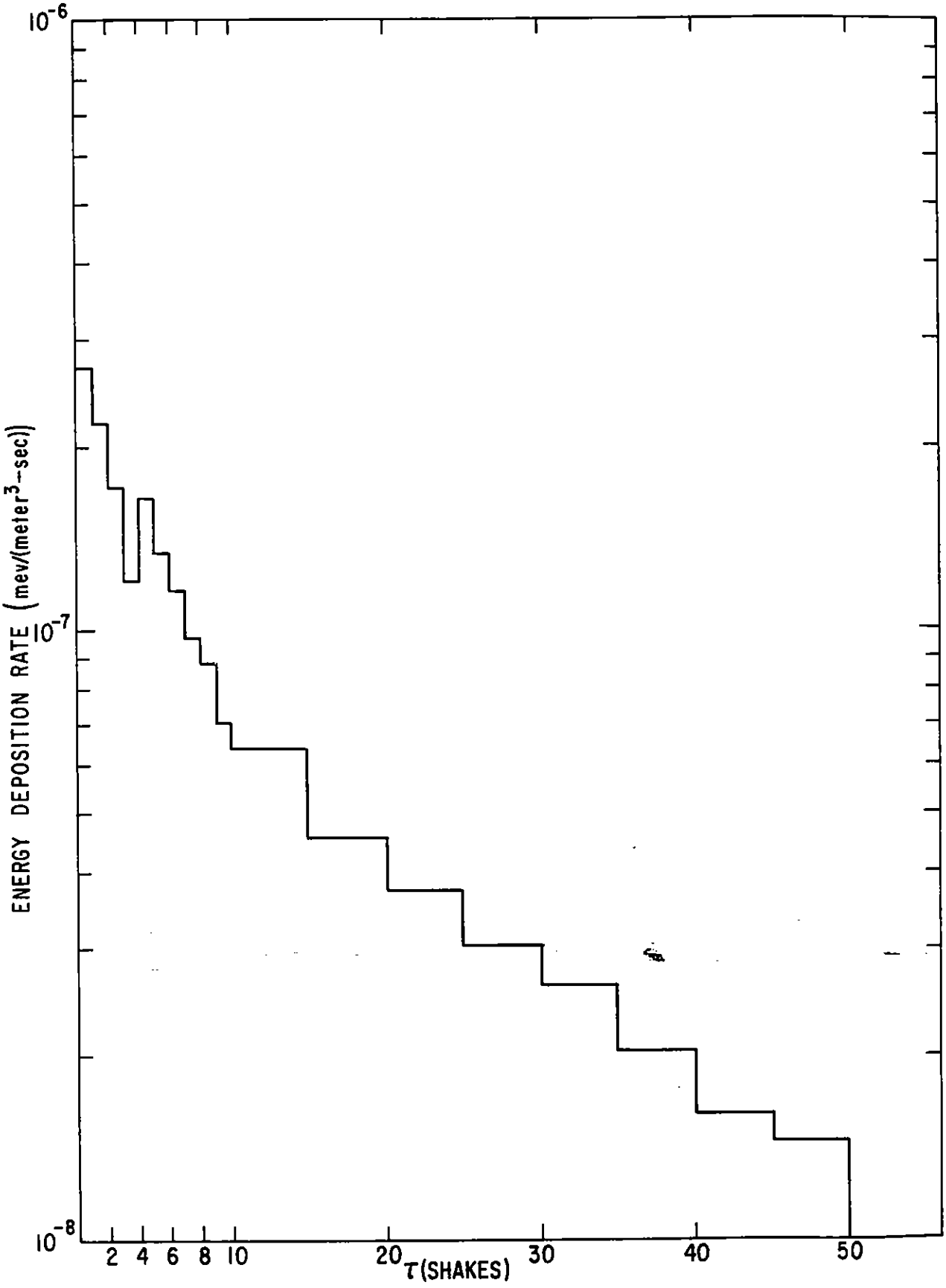

Fig. 11 Energy Deposition Rate for 4 Mev gammas at 2562.50 meters (10.02 m.f.p.)

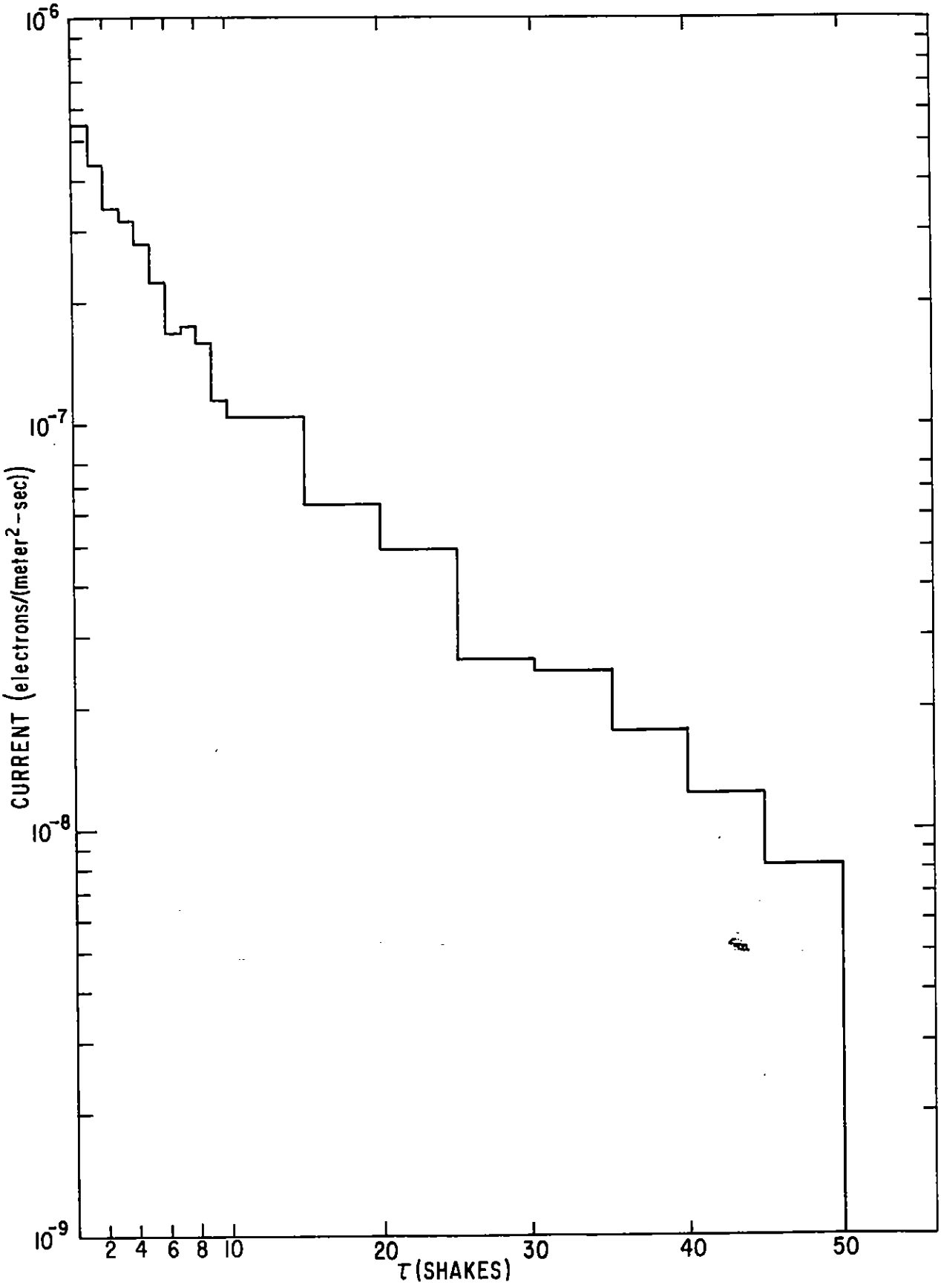

Fig. 12 Radial Current for 4 Mev gammas at 2562.50 meters (10.02 m.f.p.)

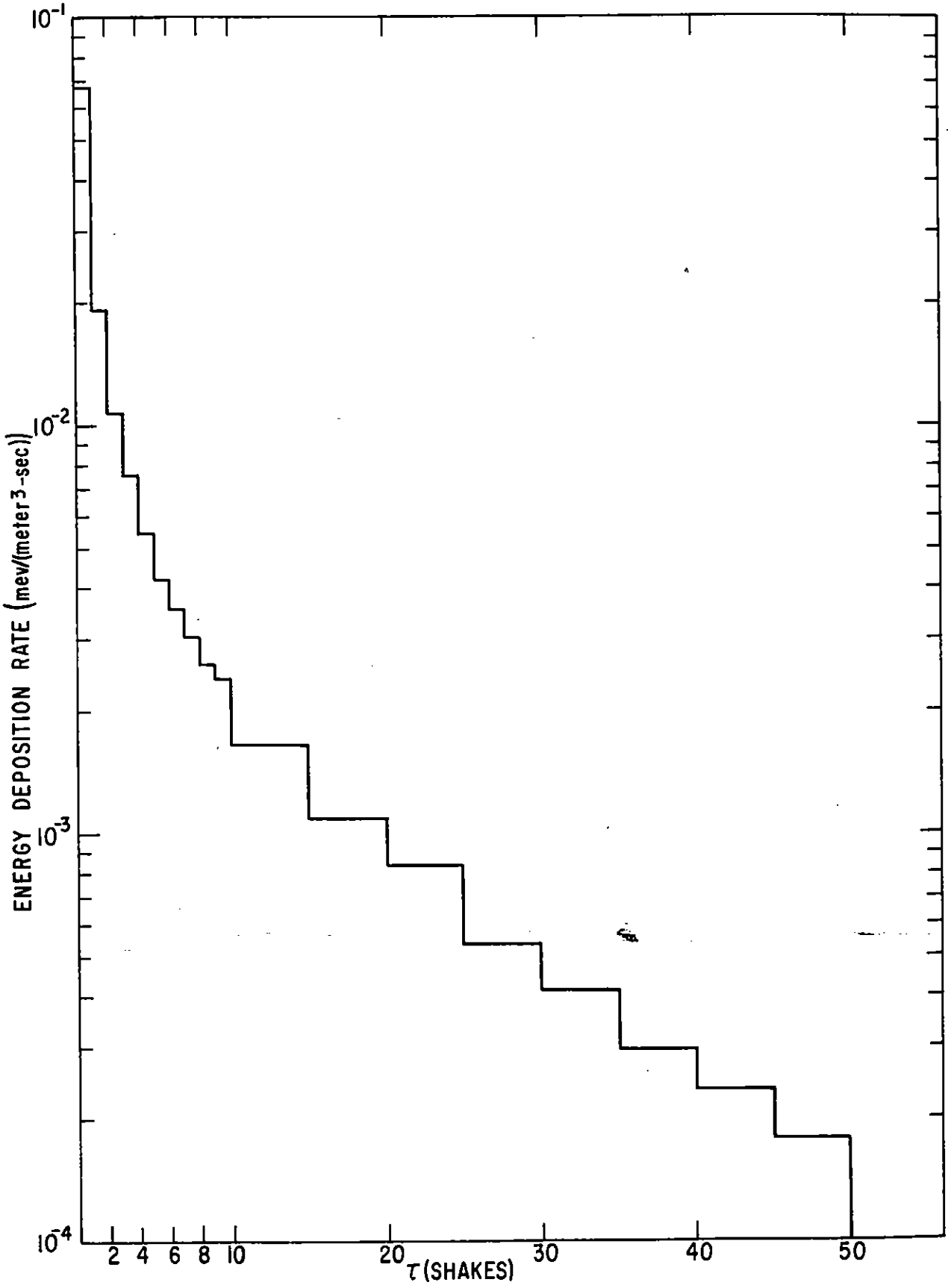

Fig. 13 Energy Deposition Rate for 8 Mev gammas at 362.50 meters (1.04 m.f.p.)

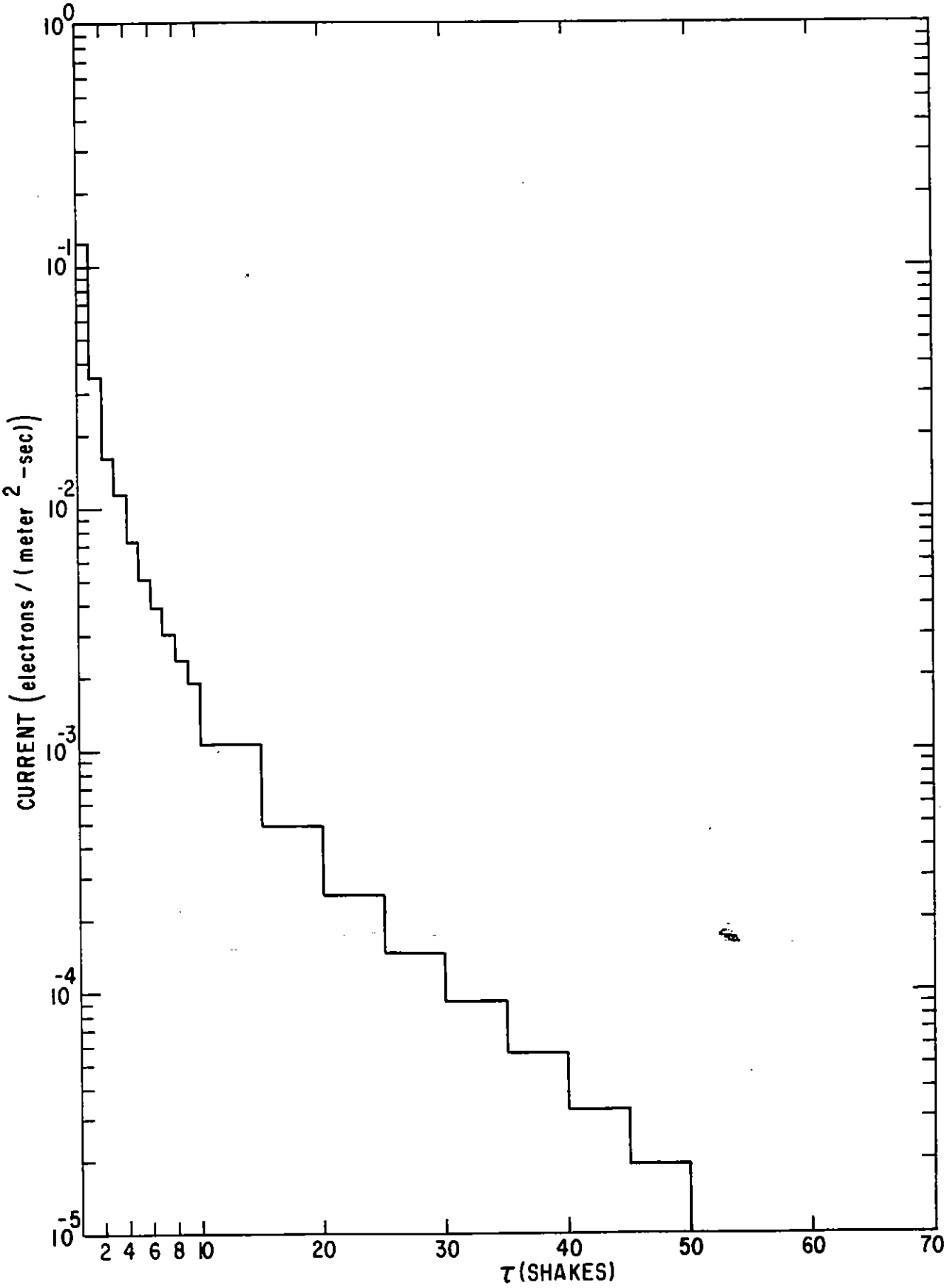

Fig. 14 Radial Current for 8 Mev gammas at 362.50 meters (1.04 m.f.p.)

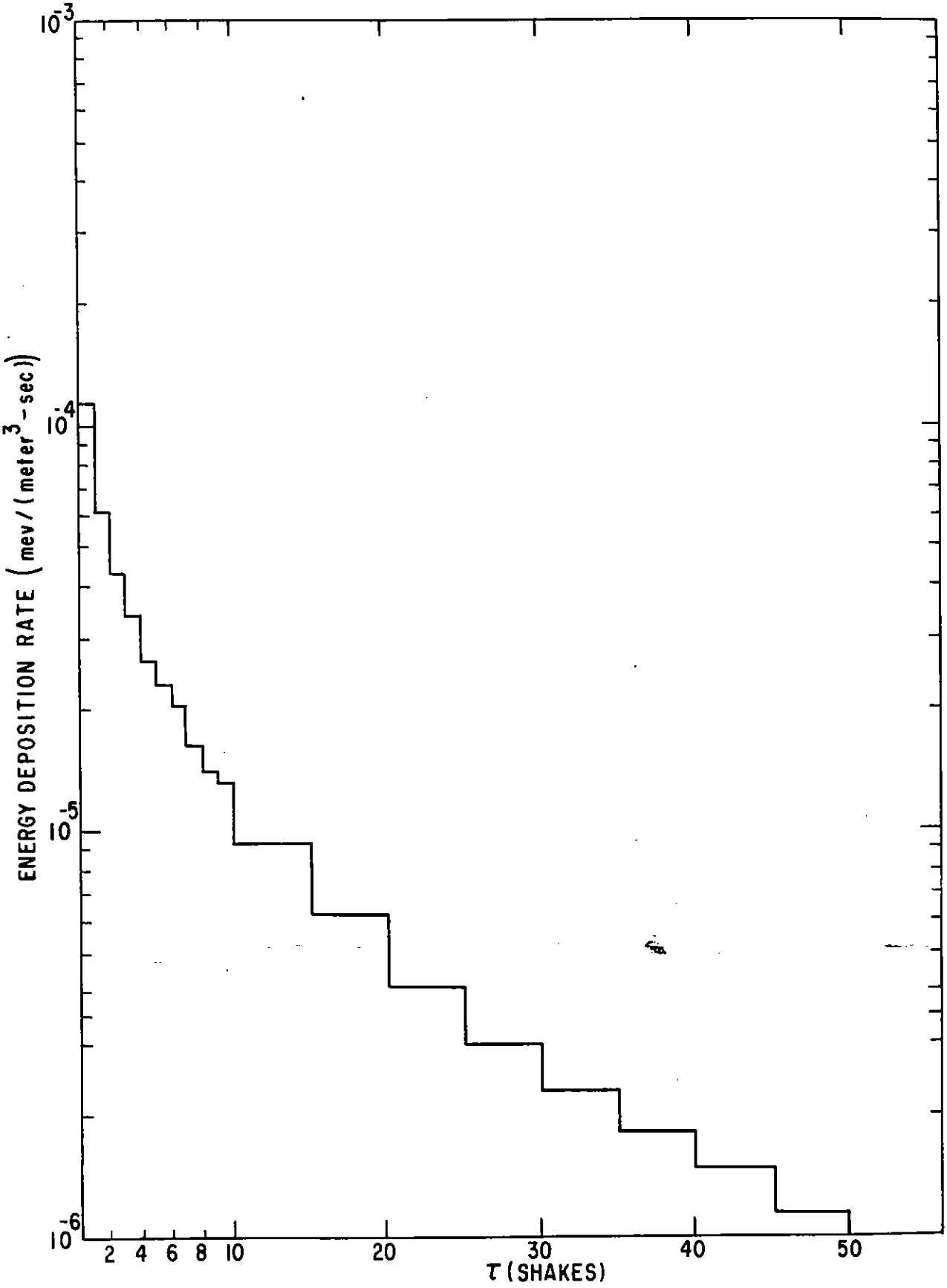

Fig. 15 Energy Deposition Rate for 8 Mev gammas at 1737.50 meters (4.98 m.f.p.)

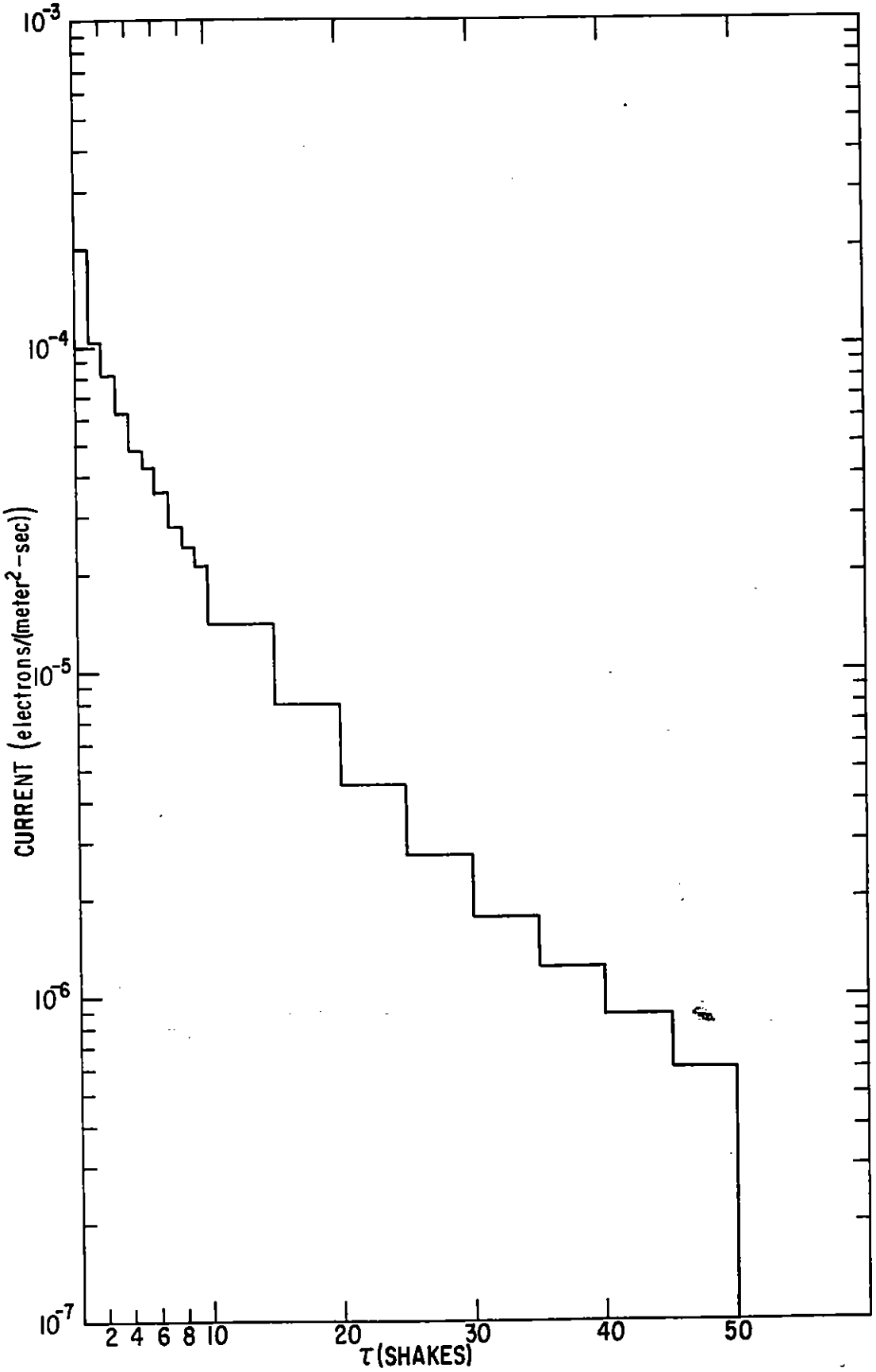

Fig. 16 Radial Current for 8 Mev gammas at 1737.50 meters (4.98 m.f.p.)

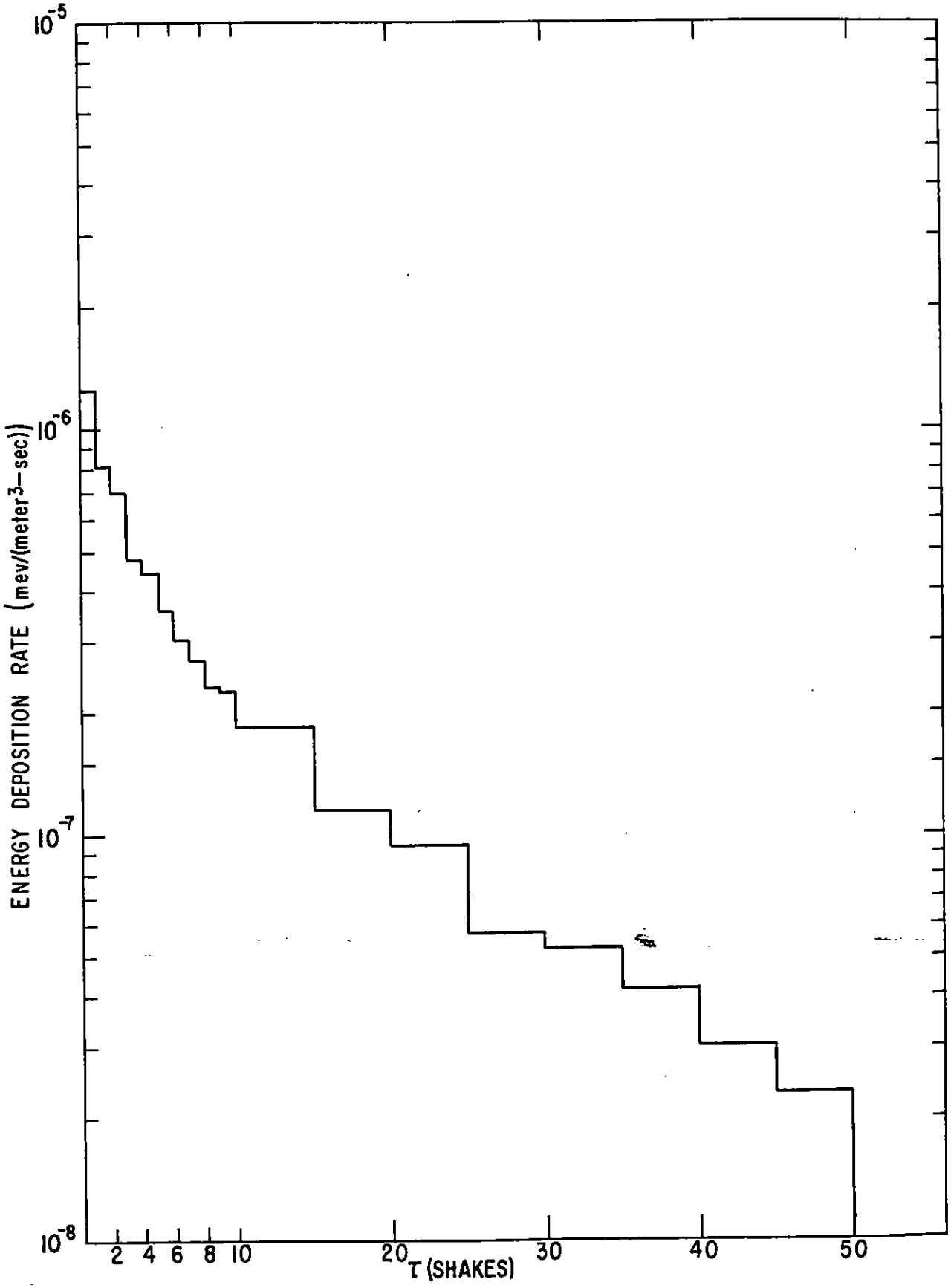

Fig. 17 Energy Deposition Rate for 8 Mev gammas at 2987.50 meters (8.56 m.f.p.)

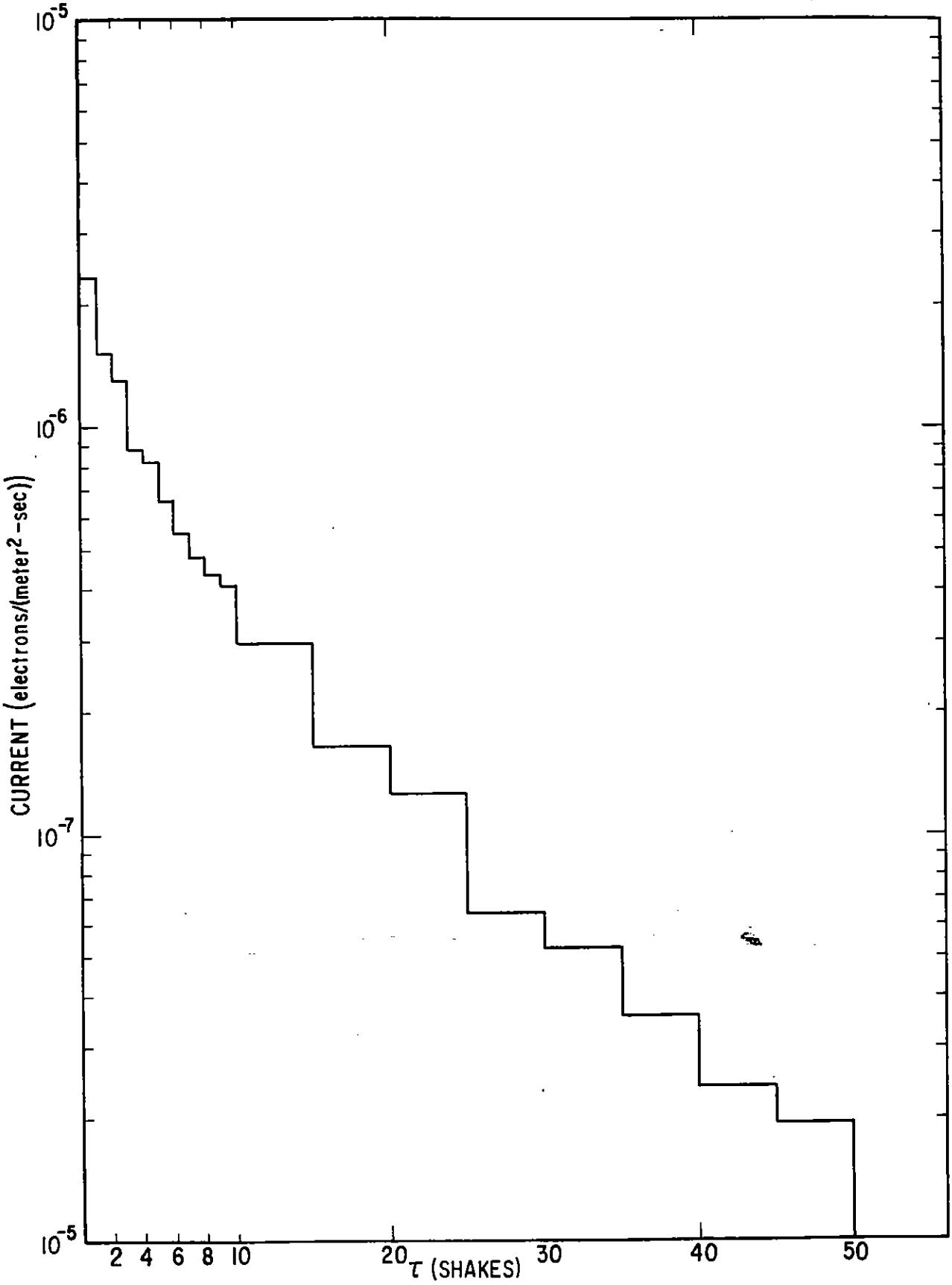

Fig. 18 Radial Current for 8 Mev gammas at 2987.50 meters (8.56 m.f.p.)

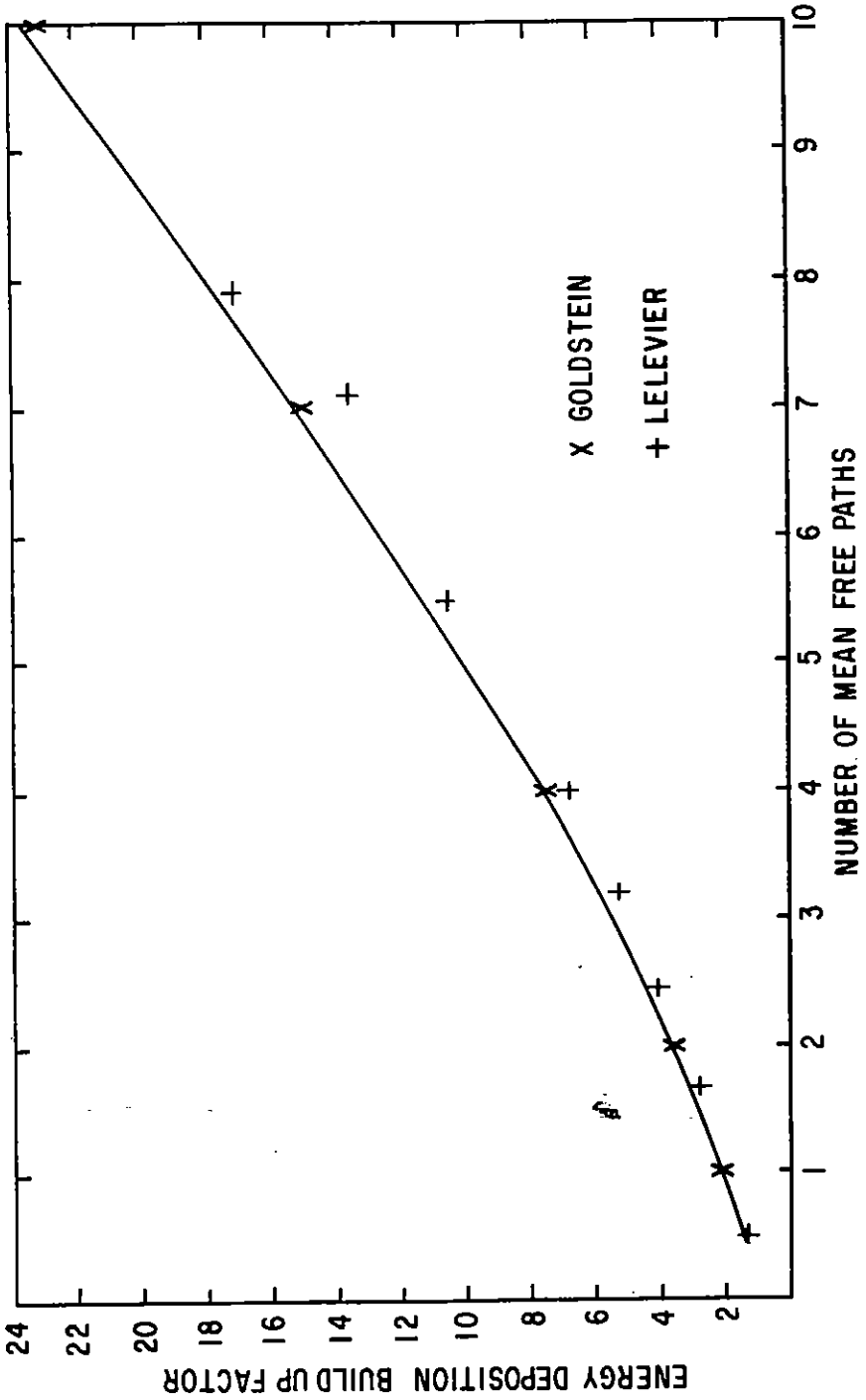

Fig. 19 Energy Deposition Buildup Factor for 1 Mev gammas as a Function of Distance from the Source

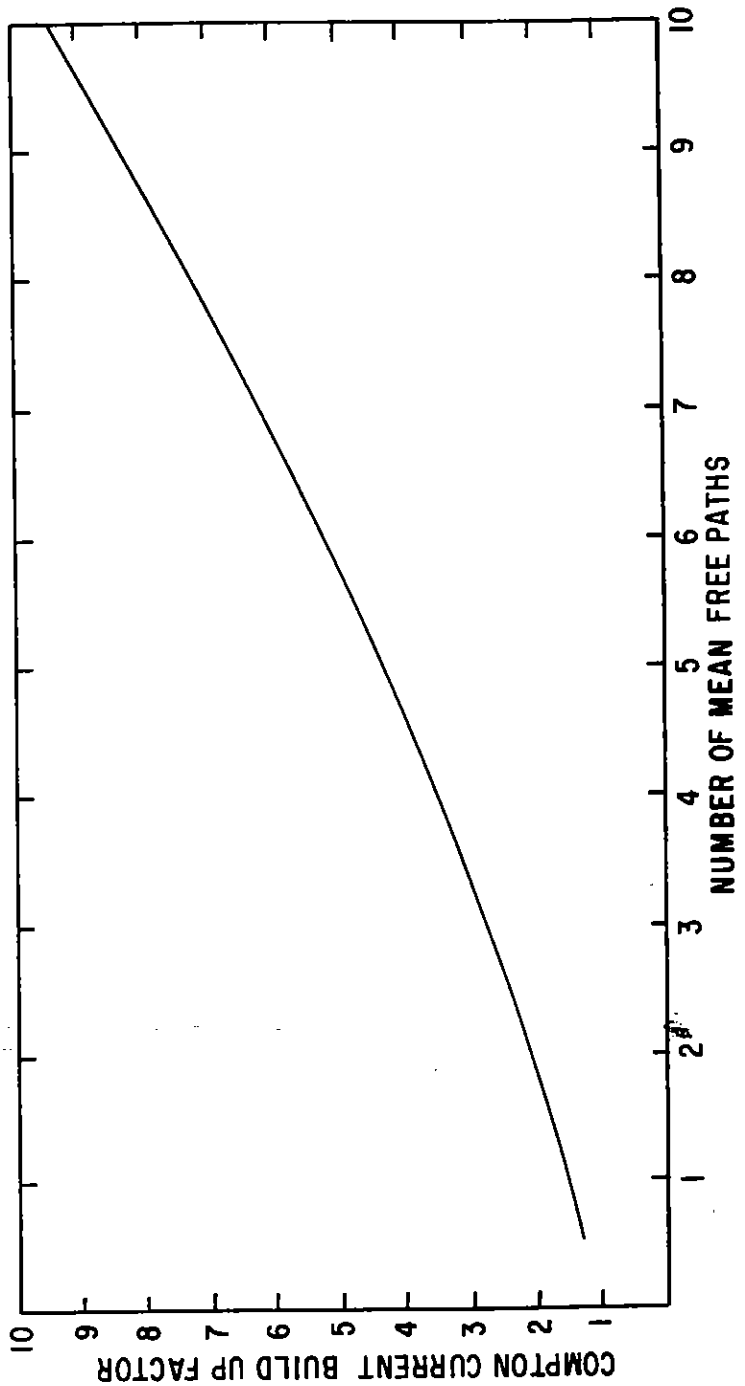

Fig. 20 Radial Current Buildup Factor for 1 Mev gammas as a Function of Distance from the Source

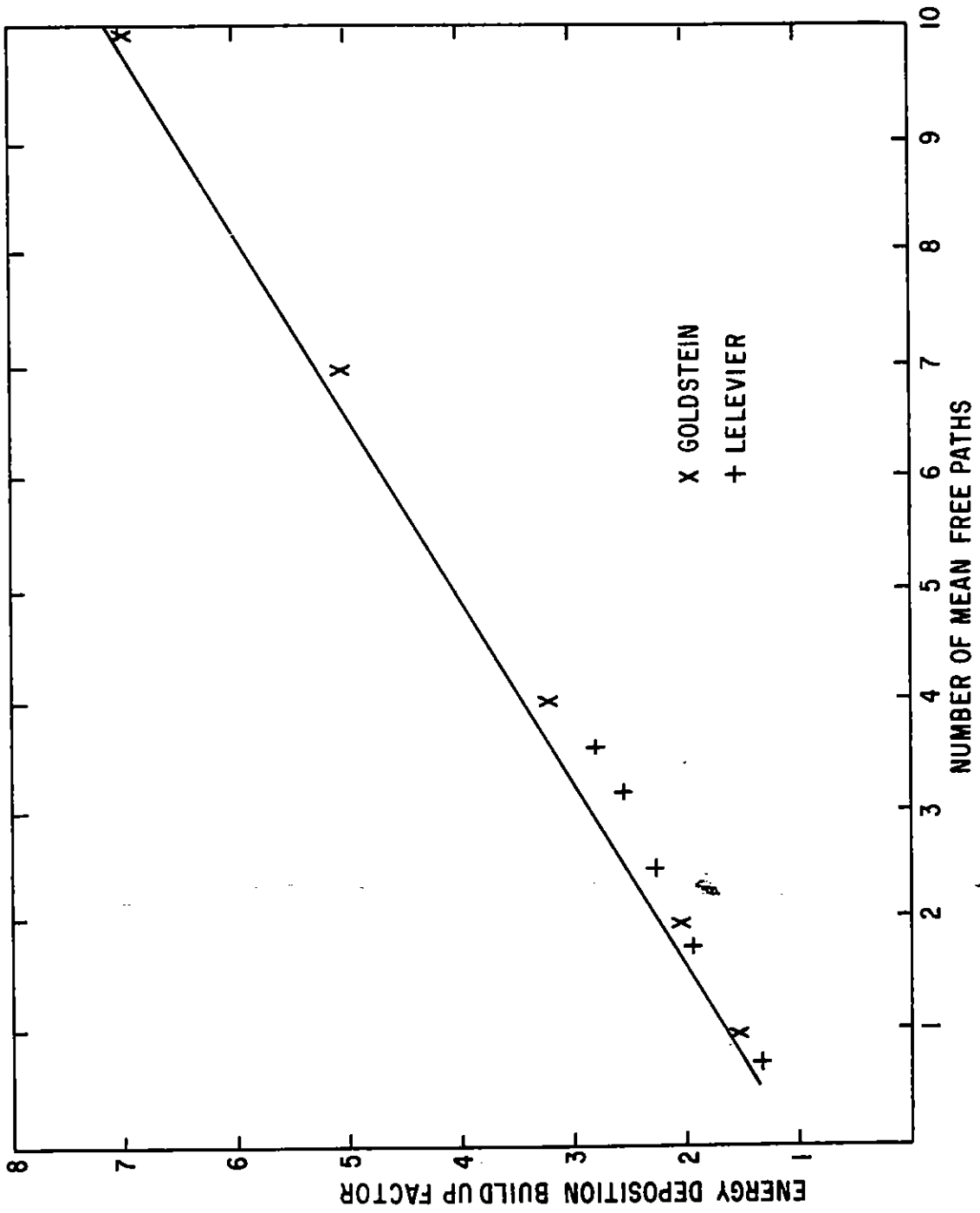

Fig. 21 Energy Deposition Buildup Factor for 4 Mev gammas as a Function of Distance from the Source

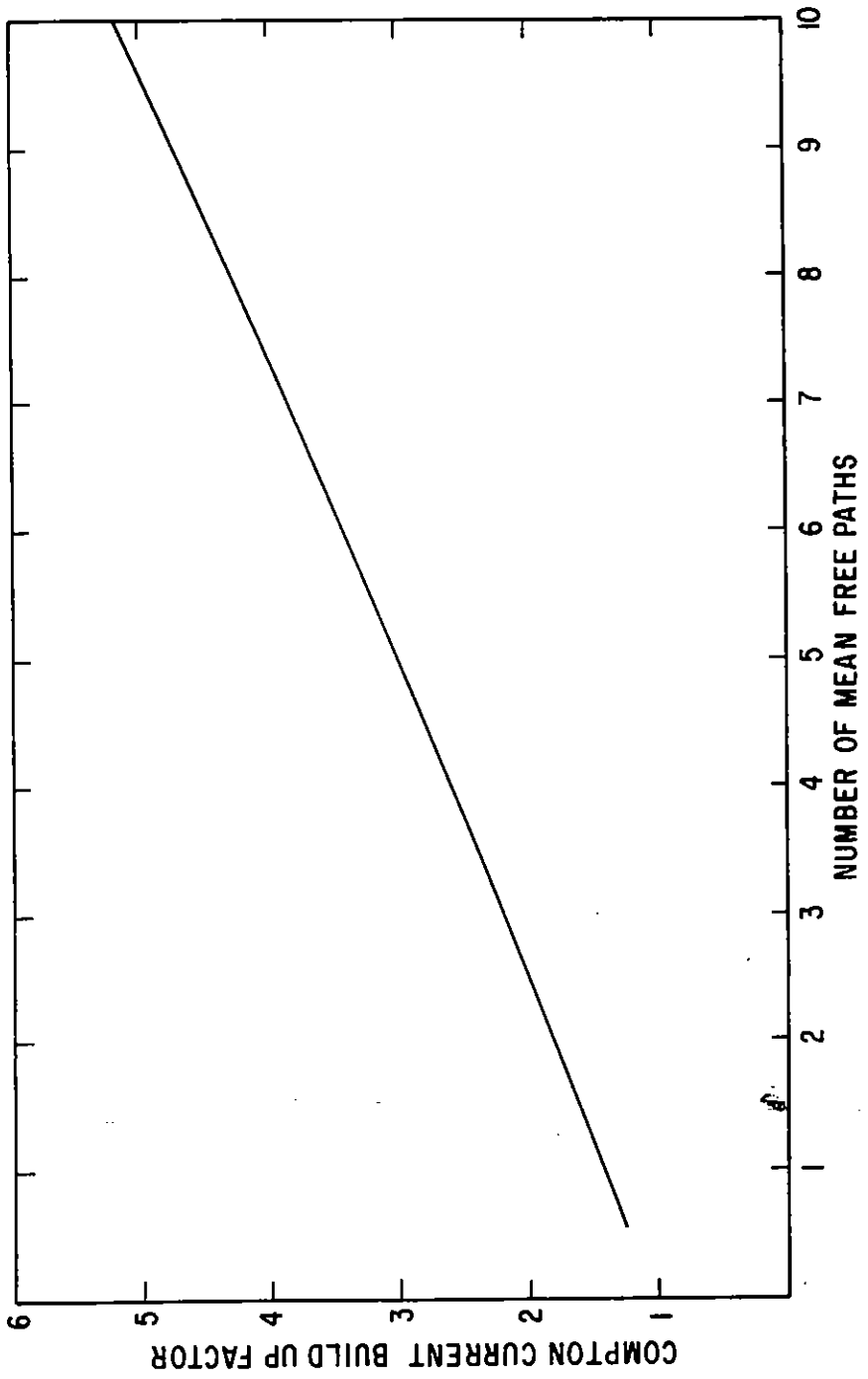

Fig. 22 Radial Current Buildup Factor for 4 Mev gammas as a Function of Distance from the Source

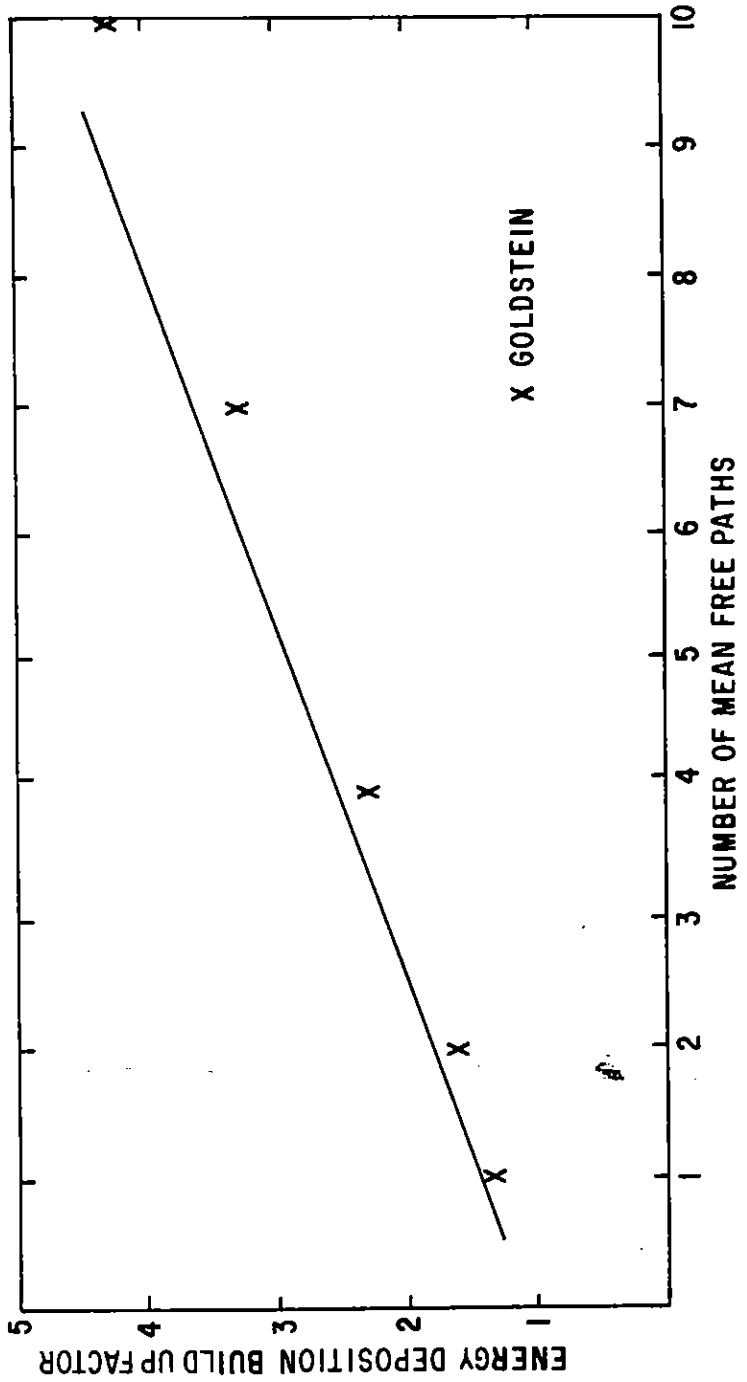

Fig. 23 Energy Deposition Buildup Factor for 8 Mev gammas as a Function of Distance from the Source

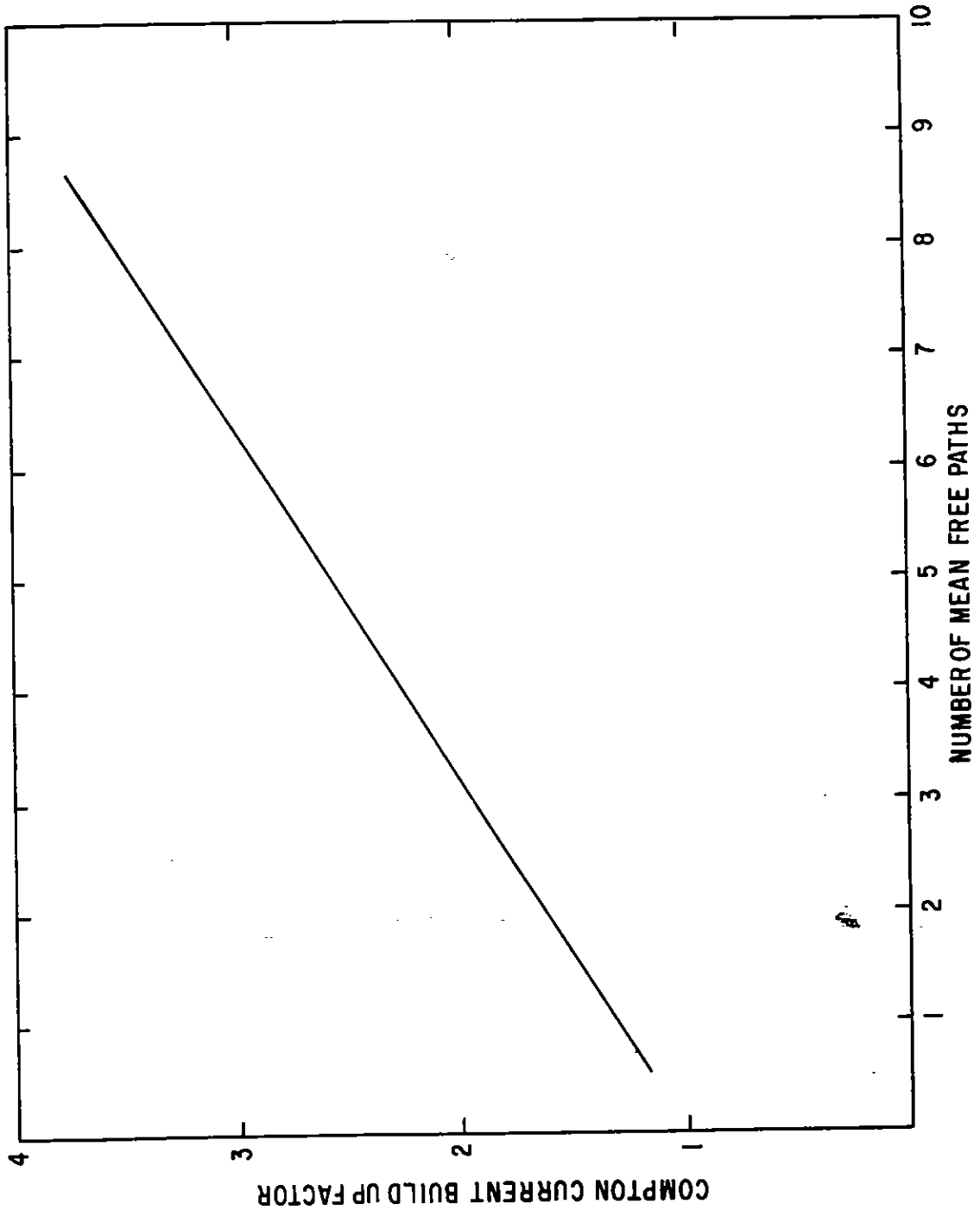

Fig. 24 Radial Current Buildup Factor for 8 Mev gammas as a Function of Distance from the Source

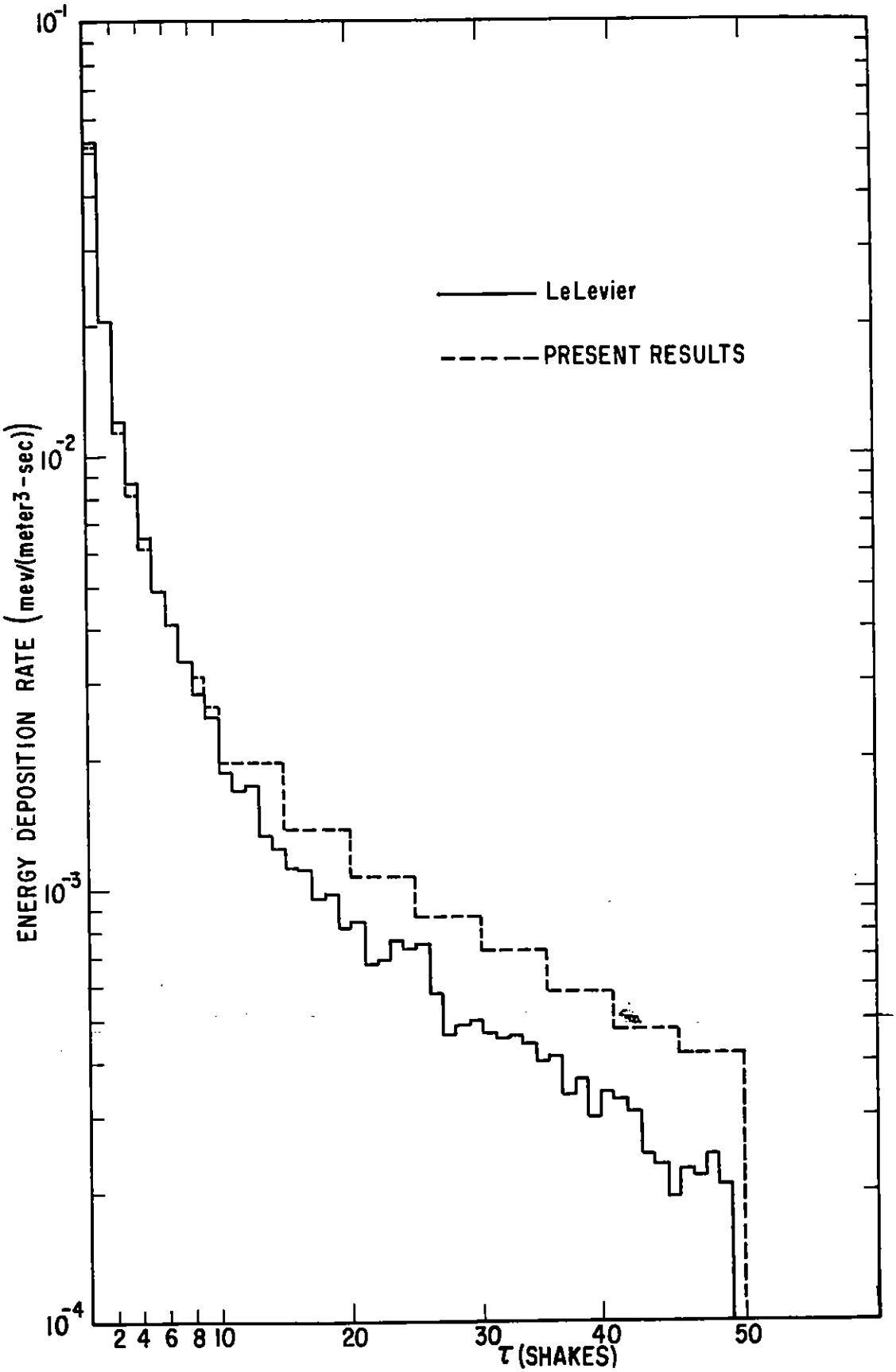

Fig. 25 Energy Deposition Rate for 4 Mev gammas at 1.10 m.f.p.

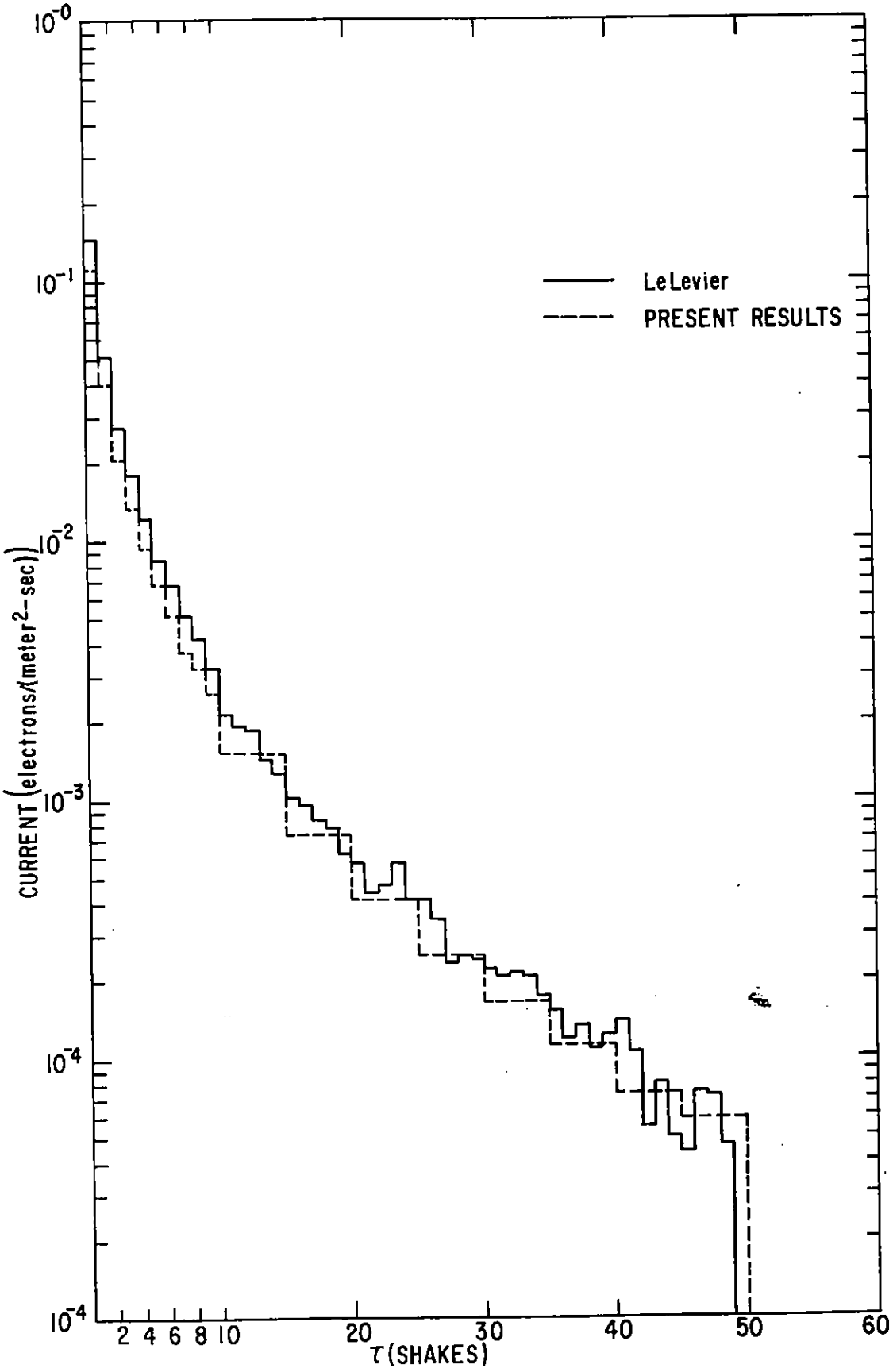

Fig. 26 Radial Current for 4 Mev gammas at 1.10 m.f.p.

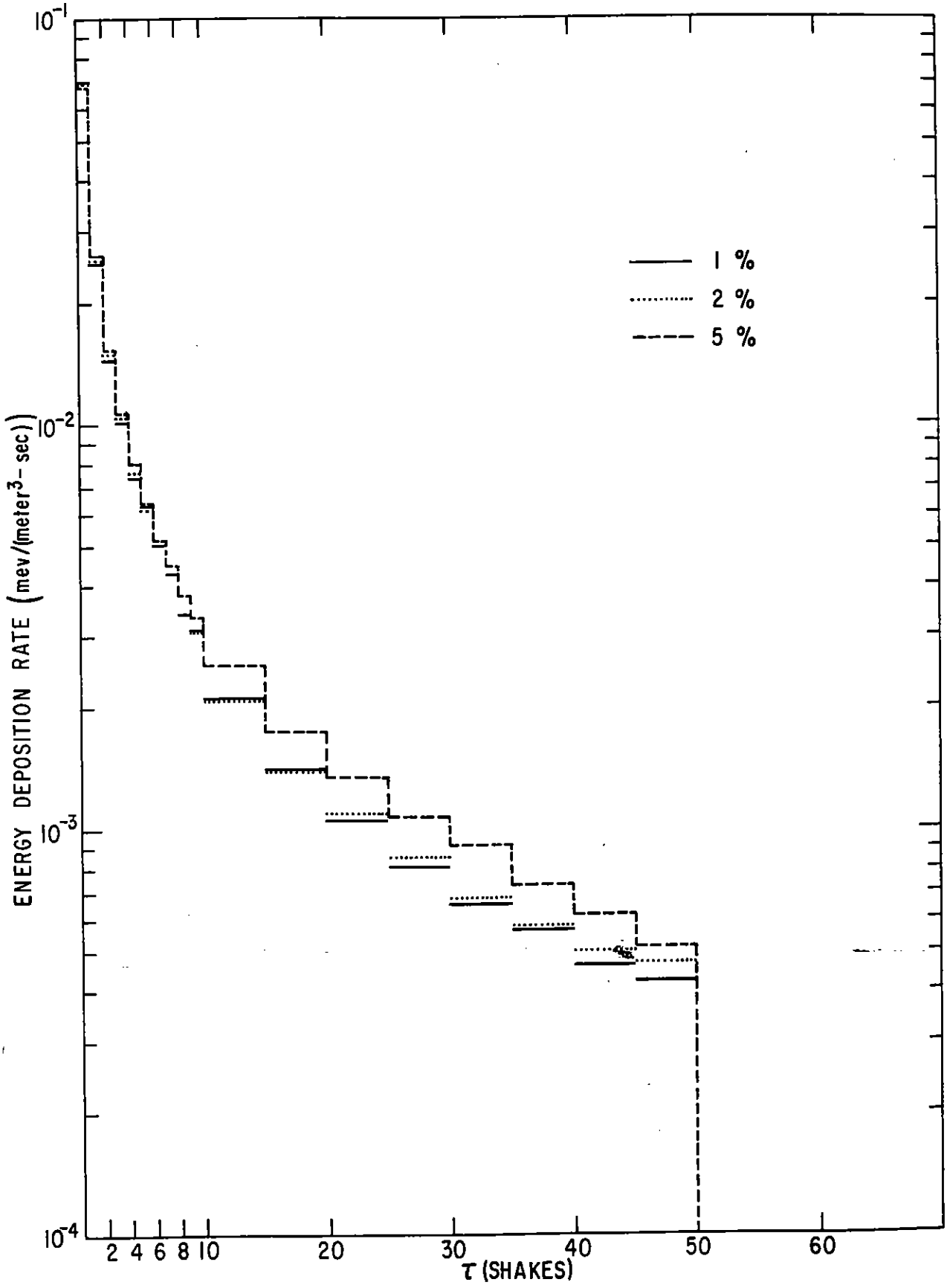

Fig. 27 Effect of Various Cutoff Energies on the Energy Deposition Rate for 4 Mev gammas at 1.12 m.f.p.

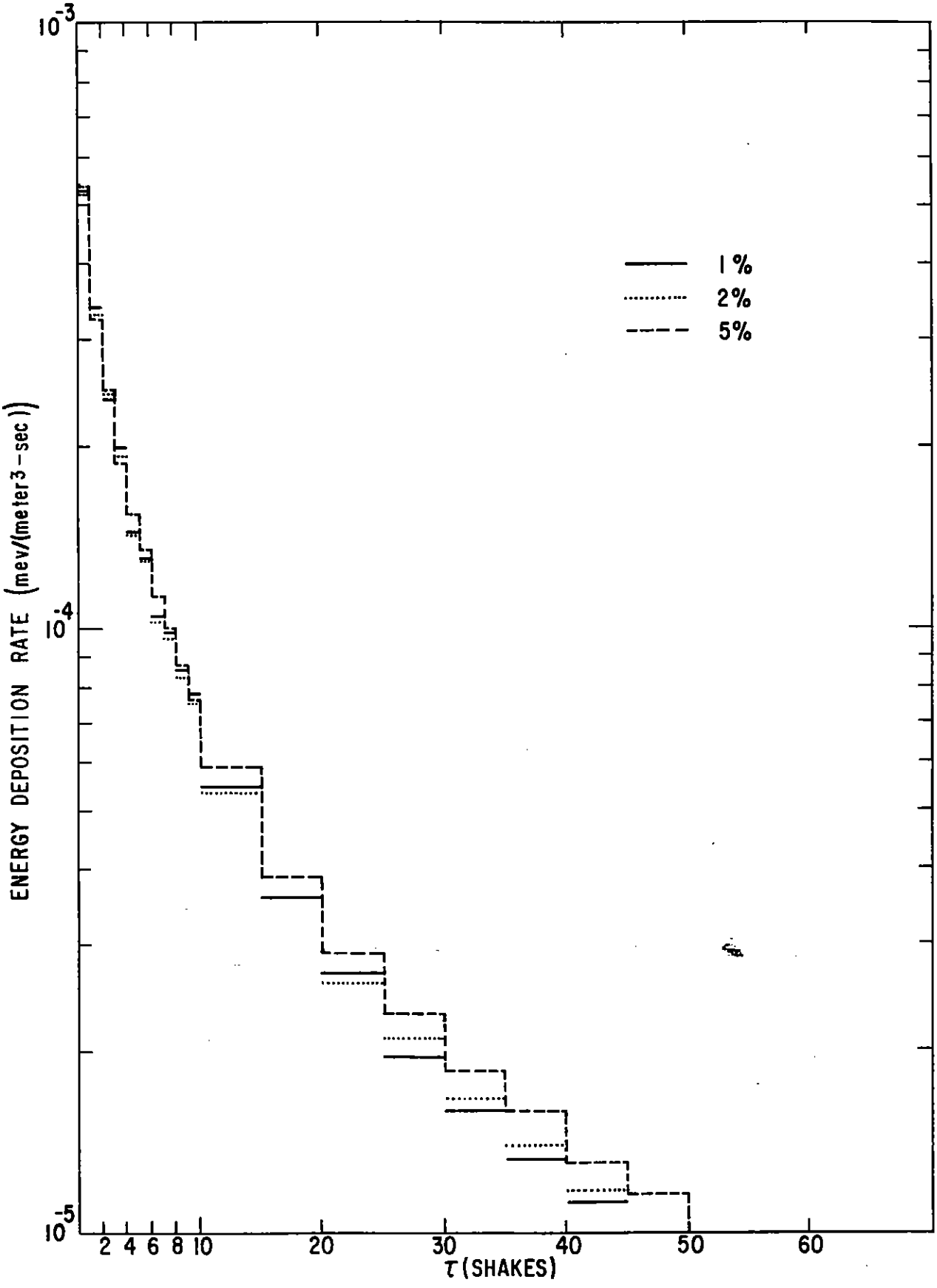

Fig. 28 Effect of Various Cutoff Energies on the Energy Deposition Rate for 4 Mev gammas at 3.96 m.f.p.

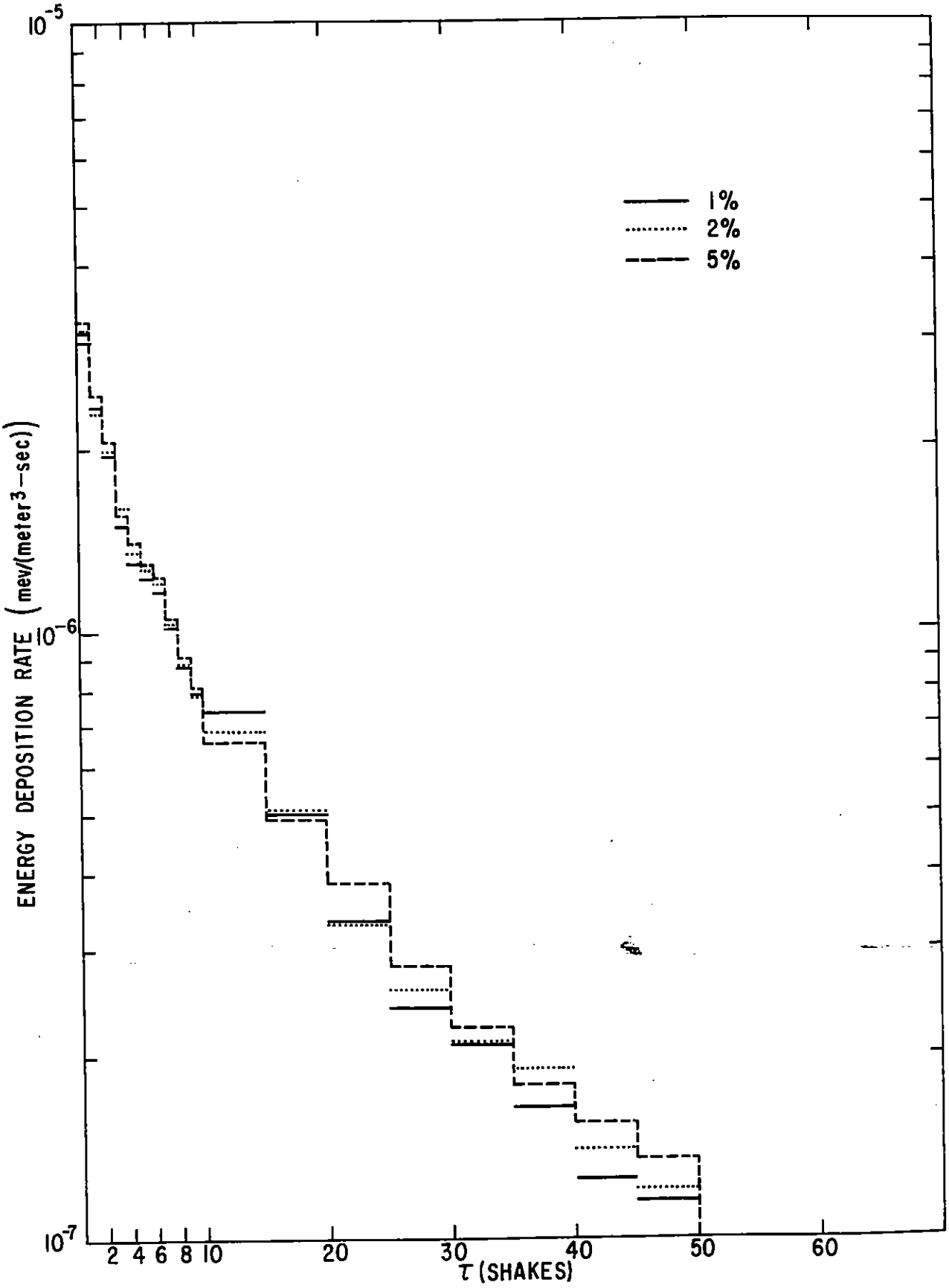

Fig. 29 Effect of Various Cutoff Energies on the Energy Deposition Rate for 4 Mev gammas at 7.87 m.f.p.